Different complement immune pathways mediate innate anxiety and learned fear

Laura J. Westacott[1,4†], Trevor Humby[1,2†], Niels Haan[1,4], Sophie A. Brain[2], Emma-Louise Bush[2], Margarita Toneva[2], Andreea-Ingrid Baloc[2], Nicola Lander[7], Anna L. Moon[1], Jack Reddaway[1,4], Michael J. Owen[1,] Jeremy Hall[1,4], Timothy R. Hughes[3,4], B. Paul Morgan[3,4,6], William P. Gray[1,4,5$] & Lawrence S. Wilkinson[1,2,4*$]

[1] Neuroscience and Mental Health Research Institute, MRC Centre for Neuropsychiatric Genetic and Genomics, School of Medicine, Hadyn Ellis Building, Cardiff University, Cardiff, CF24 4HQ, UK.[2] Behavioural Genetics Group, Schools of Psychology and Medicine, Cardiff University, Cardiff, CF10 3AT, UK. [3] Complement Biology Group, Systems Immunity Research Institute, School of Medicine, Cardiff University, CF14 4XW, Cardiff UK. [4] Hodge Centre for Neuropsychiatric Immunology, School of Medicine, Cardiff University, Cardiff CF24 4HQ, UK. [5] Brain Repair and Intracranial Therapeutics (BRAIN) Unit, School of Medicine, Cardiff University, CF24 4HQ, UK. [6] UK Dementia Research Institute, Cardiff University, Cardiff, CF24 4HQ, UK. [7] School of Biosciences, Cardiff University, Cardiff, CF10 3AT, UK.

[†] These authors contributed equally to the work
[$]Joint senior authors: Lawrence S. Wilkinson & William P. Gray

[*]Corresponding author: Lawrence S. Wilkinson

Email address: WilkinsonL@cardiff.ac.uk

Address: Neuroscience and Mental Health Research Institute, School of Medicine, Cardiff University, Cardiff, CF24 4HQ, UK

Key words: *Neuroimmunology, Behaviour, Complement system, Anxiety, Fear, Stress response.*

Abstract

Complement is a key component of the immune system with roles in inflammation and host-defence. Here we reveal unanticipated functions of complement pathways impacting on emotional reactivity of relevance to the emerging links between complement and risk for psychiatric disorder. We used mouse models to assess the effects of manipulating components of the complement system on emotionality. *C3aR*$^{-/-}$ mice demonstrated a selective increase in unconditioned (innate) anxiety whilst *C3*$^{-/-}$ mice showed a selective increase in conditioned (learned) fear. The dissociable behavioural phenotypes were linked to different signalling mechanisms. Effects on innate anxiety were independent of C3a, the canonical ligand for C3aR, indicating the existence of an alternative ligand mediating innate anxiety, whereas effects on learned fear were due to loss of iC3b/CR3 signalling. Our findings show that specific elements of the complement system and associated signalling pathways contribute differentially to heightened states of anxiety and fear commonly seen in psychopathology.

The complement system is a key component of the immune system that plays a pivotal role in inflammation and host-defence. Complement activation occurs via several pathways, all of which lead to cleavage of the central protein, C3 (see Figure S1). Activation of C3 generates the fragments C3a and C3b. C3a is an anaphylatoxin that signals via its canonical G-protein coupled receptor C3aR[1]. Activation of this receptor has been demonstrated to trigger calcium mobilization[2-4], stimulating an array of intracellular signalling pathways to induce both pro- and anti-inflammatory effects[1,5]. C3b on the other hand propagates further complement activation by contributing to the cleavage of complement component 5 (C5) downstream of C3 and, after further cleavage to iC3b, plays a role in opsonisation by macrophages and microglia via complement receptor 3 (CR3). Akin to C3, C5 cleavage generates C5a (another anaphylatoxin and a ligand for the C5a receptor, C5aR) and C5b, which triggers the terminal complement pathway by sequentially binding proteins C6, C7, C8 and C9. These proteins subsequently congregate to assemble the membrane attack complex (MAC) which ultimately results in destruction of the target cell or pathogen via cell lysis[6].

In the central nervous system evidence is emerging that complement has functions beyond its canonical immune roles[7]. Neurons, astrocytes and microglia express complement receptors and regulators, and are also capable of synthesising complement proteins[8,9]. The expression patterns of these vary over the course of brain development[10]. Complement impacts a number of neurodevelopmental processes including neurogenesis[11], migration[12] and synaptic pruning[13] as well as ongoing synaptic plasticity processes underlying learning and memory in the adult brain[14]. Furthermore, there is increasing evidence that complement is causally involved in the

93 pathogenesis of neurodegenerative and psychiatric conditions. In Alzheimer's
94 disease, genetic variants in complement related loci have been associated with
95 increased disease risk[15,16], and complement knockout mice exhibit reduced age-
96 related synapse loss[17] and neuropathology[18]. Alterations in complement proteins and
97 activation have also been reported in sera from individuals with autism-spectrum
98 disorder[19] schizophrenia[20], major depressive disorder[21], bipolar disorder[22] and post-
99 traumatic stress disorder[23].
100
101 In the case of schizophrenia, an important finding comes from elegant genetic work
102 demonstrating that structural variation in the *C4* locus is associated with risk of
103 developing the disease[24]. C4 cleavage generates fragments that contribute to the
104 activation of C3, yielding C3a and C3b. Given the known roles for the iC3b/CR3
105 pathway in developmental synaptic pruning[13,25], it has been suggested that *C4*
106 variants may impact on psychiatric risk via this mechanism, with excessive synaptic
107 elimination leading to abnormal connectivity and disruption of neural networks[24].
108 Variants in *C3* and putative complement-control genes *CSMD1* and *CSMD2* have also
109 been implicated in genetic susceptibility for schizophrenia[26,27].
110
111 Altered emotional function, in particular maladaptive anxiety and fear, is a pervasive
112 and clinically important symptom that is comorbid across several of the DSM-5 and
113 ICD-11 defined disorders in which complement has been implicated. Anxiety and fear
114 are distinct aversive states elicited by differing environmental factors, that result in
115 distinguishable behavioural outputs[28]. Anxiety is characterised by sustained arousal,
116 hypervigilance and risk assessment surrounding anticipated or potential threats, while
117 fear is an acute response to an experienced, imminent danger resulting in immediate

118 avoidance, fight or freezing behaviour[29,30]. Whilst there is significant overlap in the
119 neurocircuitry underlying these states, there are also contributions from distinct
120 neuronal circuitries[28,31]. Although links between anxiety and inflammation have been
121 documented[32], there has been little investigation of the specific role of complement in
122 either anxiety or fear. In animal models, anxiety phenotypes arise from heightened
123 pre-natal complement activity[33] and complement inhibitors reduce anxiety associated
124 with neurodegeneration[34]. Furthermore, aged *C3* deficient mice exhibited lower levels
125 of anxiety alongside enhanced contextual fear responses[17]. These latter studies
126 suggest that complement can influence both innate and learned components of
127 aversive behaviours, however, the precise relationship between signalling within
128 discrete pathways of the complement system and their relationship to dissociable
129 aspects of emotionality and underlying brain function is unknown.
130
131 Utilising the central role of C3 in complement signalling, we used a combination of
132 complement knockout mice to functionally parse anxiety and fear related phenotypes.
133 In homozygous *C3* knockout mice ($C3^{-/-}$)[35] complement cannot be activated beyond
134 C3, and therefore these animals lack C3 activation fragments (C3a, C3b) and
135 downstream activation products (C5a, C5b) and thus cannot activate the terminal
136 complement pathway. Phenotypes in this model could therefore be the result of loss
137 of any of these downstream effector molecules. We compared the $C3^{-/-}$ model with
138 homozygous *C3aR* knockout mice ($C3aR^{-/-}$)[36]. In these mice, complement is intact
139 apart from the capacity for C3a to bind its canonical receptor C3aR and hence we
140 tested the extent to which phenotypic effects were the result specifically of disrupted
141 C3a/C3aR signalling. A priori, because C3a is an obligate cleavage fragment of C3,

142 we hypothesised that any phenotypes dependent on the binding of C3a to C3aR would
143 be apparent in both *C3*$^{-/-}$ and *C3aR*$^{-/-}$ models.
144
145 Contrary to our hypotheses we found clear phenotypic dissociations between the *C3*$^{-}$
146 $^{/-}$ and *C3aR*$^{-/-}$ models which were dependent on the nature of the emotional behaviour.
147 *C3aR*$^{-/-}$ mice displayed a profound innate anxiety phenotype that was lacking in the
148 *C3*$^{-/-}$ model. In contrast, when we examined learned fear, where a previously neutral
149 cue generates a fear response as a result of predicting an aversive outcome, we found
150 that the dissociation was reversed with the *C3*$^{-/-}$ mice exhibiting an enhanced fear
151 response to a conditioned cue, but no differences between wildtype and *C3aR*$^{-/-}$mice.
152 This observed double dissociation in emotionality was linked to distinct underlying
153 complement signalling mechanisms, with anxiety phenotypes in C3aR mice likely to
154 be independent of C3a/C3aR signalling raising the possibility of an alternative ligand
155 for C3aR, and *C3*$^{-/-}$ effects on learned fear the result of alterations in iC3b-CR3
156 pathway activity. These findings point to a hitherto unrecognized complexity of
157 complement effects on brain function and behaviour of relevance to emotional
158 dysfunction in psychopathology.
159
160 **Results**
161 **Increased innate anxiety in *C3aR*$^{-/-}$ but not *C3* $^{-/-}$ mice**
162 Full details of the complement knockout models used can be found in the Methods.
163 Using a cohort of male wildtype, *C3*$^{-/-}$ and *C3aR*$^{-/-}$ mice we first assessed emotional
164 reactivity in the elevated plus maze (EPM), a well-established test of innate anxiety in
165 rodents which exploits the conflict between the drive to explore novel environments
166 and the innate aversion towards open, brightly lit spaces[37,38]. Heatmaps indexing

167 overall maze exploration over a 5-minute session demonstrated major differences in
168 open arm exploration between genotypes (Figure 1A; see Supplementary Video 1 for
169 representative examples). Notably, in comparison to wildtype and *C3*$^{-/-}$ mice, *C3aR*$^{-/-}$
170 mice took significantly longer to first enter the open arms (Figure 1B) and spent less
171 time on the open arm per entry (Figure S2A), leading to a reduced overall duration
172 spent in the open arms (Figure 1C), findings consistent with increased anxiety. The
173 ethological parameters head dips and stretch attend postures (SAPs) also differed
174 between genotypes (Figure 1D,E), with *C3aR*$^{-/-}$ mice exhibiting decreases in the
175 former and increases in the latter, a pattern of results again consistent with heightened
176 anxiety[39]. We also noted a significantly increased frequency of head dipping in *C3*$^{-/-}$
177 mice (Figure 1D), consistent with reduced levels of anxiety relative to both wildtype
178 and *C3aR*$^{-/-}$ mice[40].
179
180 These initial data were consistent with an anxiogenic phenotype present in *C3aR*$^{-/-}$
181 mice but absent in *C3*$^{-/-}$ mice. We confirmed the findings in two further independent
182 tests of anxiety using additional cohorts of animals. First we used the elevated zero
183 maze (EZM, see Methods), another test of anxiety-like behaviour which similarly
184 probes behavioural responses to exposed, illuminated spaces[41]. The data
185 recapitulated the pattern of findings seen in the EPM (Figure 1F-J). Additional data
186 from the open field test, where *C3aR*$^{-/-}$ mice were more likely to avoid the centre of the
187 arena, were also consistent in demonstrating a specific anxiety-like phenotype in
188 *C3aR*$^{-/-}$ but not *C3*$^{-/-}$ mice (Figure S3). Given that several of the measures indexing
189 anxiety were dependent on movement around the apparatus it was important to
190 eliminate potential locomotor confounds. To address this issue, we measured activity
191 independently in a non-anxiety provoking environment and found no differences in

192 locomotor activity between genotypes (Figure S2C), demonstrating that anxiety
193 measures were not influenced by movement confounds.
194
195 **Neuroendocrine response and neuronal activation in *C3aR*$^{-/-}$ and *C3*$^{-/-}$ mice**
196 **following exposure to the elevated plus maze**
197 We next tested whether the behavioural measures of anxiety were paralleled by
198 changes in plasma levels of the stress hormone corticosterone. In a separate cohort
199 of wildtype, *C3*$^{-/-}$ and *C3aR*$^{-/-}$ mice, we assayed plasma corticosterone 30 minutes after
200 exposure to the EPM and compared levels to those of a group of animals who
201 remained in their home-cages. There were no genotype differences in basal
202 corticosterone levels; however, being placed on the EPM increased plasma
203 corticosterone 6-15-fold in all genotypes, demonstrating that the EPM was a potent
204 stressor (Figure 2A). *Post hoc* analyses showed a significantly greater EPM-evoked
205 corticosterone response in the *C3aR*$^{-/-}$ animals, consistent with their increased
206 anxiety-like behaviour observed on the maze.
207
208 Neuronal activity within the ventral hippocampus (vHPC) has been linked to anxiety in
209 rodents[42,43] therefore we also investigated mRNA expression of two immediate early
210 genes (IEGs), *c-Fos* and *zif268,* in a further cohort of behaviourally naïve wildtype,
211 C3$^{-/-}$ and C3aR$^{-/-}$ animals. There were no effects on *zif268* expression but 5-minute
212 exposure to the EPM was found to significantly increase *c-Fos* expression 30 minutes
213 later, compared to animals who remained in their home-cages (Figure 2B). In wildtype
214 animals there was a 4.95-fold increase in *c-Fos* expression over baseline and
215 increases in EPM-evoked *c-Fos* expression in *C3*$^{-/-}$ and *C3aR*$^{-/-}$ models of 7.77-fold
216 and 6.54-fold, respectively (Figure 2B). Thus, whilst being placed on the EPM led to

217 significant general increases in *c-Fos* in vHPC, the enhanced activity seen in the
218 knockout models did not differentiate between *C3*$^{-/-}$ and *C3aR*$^{-/-}$ and did not predict the
219 observed dissociations in anxiety-related behaviours.
220
221 **Altered sensitivity of *C3aR*$^{-/-}$ and *C3*$^{-/-}$ mice to diazepam in the elevated plus maze**
222 In a further independent cohort of animals, we tested the sensitivity of EPM induced
223 anxiety-like behaviour to the benzodiazepine diazepam, an established clinically
224 effective anxiolytic drug[37,44]. Our initial behavioural findings were replicated in vehicle-
225 treated animals across all behavioural indices of anxiety, again showing an anxiogenic
226 phenotype in *C3aR*$^{-/-}$ but not *C3*$^{-/-}$ mice (Figure 3A). As anticipated, in wildtype mice
227 2mg/kg diazepam led to a trend for increased time on the open arms (Figure 3B) and
228 a significant reduction in SAPs which are considered to reflect risk assessment
229 behaviour[45-47](Figure 3C). These effects were therefore consistent with reduced
230 anxiety[40,47]. In contrast, the same dose of drug that was effective in eliciting anxiolysis
231 in wildtypes was without effects in *C3aR*$^{-/-}$ mice (Figure 3A,B,C) and produced a
232 seemingly anxiogenic (increased anxiety) pattern of effects in *C3*$^{-/-}$ mice (Figure 3A,B
233 and Figure S4B,C). Locomotor activity monitored across all the maze (Figure S4D)
234 indicated that wildtype and *C3aR*$^{-/-}$ mice were unlikely to have been influenced by
235 diazepam-induced sedation. In *C3*$^{-/-}$ mice however, activity was significantly
236 suppressed under drug conditions indicating a possible sedative effect. Together,
237 these data indicated a fundamentally altered reactivity to diazepam in both *C3*$^{-/-}$ and
238 *C3aR*$^{-/-}$ models.
239
240
241

242 **Enhanced fear learning in *C3*$^{-/-}$ but not *C3aR*$^{-/-}$ mice**

243 Psychiatric disorders are associated with maladaptive responses to both innate,
244 unconditioned and learned aversive stimuli[48,49]. We therefore extended our analysis
245 to investigate whether the behavioural dissociations in innate anxiety observed
246 between *C3*$^{-/-}$ and *C3aR*$^{-/-}$ mice would also apply to learned or conditioned fear, where
247 a previously neutral cue generates a fear response as a result of predicting an aversive
248 outcome. In a further group of animals, we used the fear-potentiated startle (FPS)
249 paradigm[30,50] a well-established method of generating learned fear responses to an
250 acute and imminent danger signal that is characteristic of fear. In this paradigm (see
251 Figure 4A and Methods) fear learning is indexed by an enhanced response to a
252 startling noise in the presence of a cue (the conditioned stimulus or CS) previously
253 paired with mild foot shock (the unconditioned stimulus). In the pre-conditioning
254 session, pulse-alone trials revealed increased basal startle reactivity in both *C3aR*$^{-/-}$
255 and *C3*$^{-/-}$ animals relative to wildtype (Figure 4B). Increased reactivity to the
256 unconditioned foot shock stimulus (in the absence of any startle stimulus) during the
257 conditioning session was also observed in both knockouts (Figure 4C). However,
258 these common effects of genotype were not seen in the fear-potentiated startle
259 measures which index fear learning. Whilst all groups showed the expected
260 enhancement of the startle response in the presence of the CS, the effect of the CS
261 was significantly greater in *C3*$^{-/-}$ animals relative to the *C3aR*$^{-/-}$ and wildtype animals
262 (Figure 4D), indicating enhanced learning of the fear related-cue by the *C3*$^{-/-}$ mice.
263 This was the opposite pattern of effects to those observed in the tests of innate anxiety
264 and showed a double dissociation in the impact of manipulating C3 and C3aR function
265 that depended fundamentally on the nature of the aversion.

266

267 **Complement signalling pathways underlying abnormal learned fear phenotypes**
268 **in *C3*$^{-/-}$ mice**

269 Given the central role of C3 within the complement system, its deletion affects a
270 number of distal pathways (Figure 5A), with the activity of the C3a/C3aR, C3b/CR3,
271 C5a/C5aR and terminal pathways affected. Therefore, the loss of function of any of
272 these pathways may have contributed to the observed fear learning phenotype in *C3*$^{-}$
273 $^{/-}$ mice. However, it is possible to exclude effects due to loss of the C3a/C3aR pathway
274 since the fear learning phenotype was specific to *C3*$^{-/-}$ and not *C3aR*$^{-/-}$ mice (Figure
275 4D). This left iC3b/CR3 signalling and/or pathways downstream of C5 (i.e. C5a/C5aR,
276 terminal pathway) as the remaining possibilities. In order to distinguish between these
277 pathways, we repeated the FPS experiment with the addition of *C5*$^{-/-}$ mice. This model
278 has intact C3a/C3aR and iC3b/CR3 signalling, but lacks C5a/C5b and terminal
279 pathway activity, as do *C3*$^{-/-}$ mice. We hypothesised that if C*5*$^{-/-}$ mice also displayed
280 enhanced fear-potentiated startle, then the phenotype in *C3*$^{-/-}$ mice would likely be due
281 to a loss of C5a/C5aR signalling or the terminal pathway. On the other hand, if *C5*$^{-/-}$
282 mice demonstrated normal fear-potentiated startle, this would confine the likely
283 mediating pathway in *C3*$^{-/-}$ mice to iC3b/CR3 signalling.
284

285 Results from the pre-conditioning session demonstrated increases in the startle
286 response of C*5*$^{-/-}$ mice, (Figure 5B) although in this instance the previously observed
287 enhanced startle reactivity in C*3*$^{-/-}$ mice (Figure 4B) was not replicated. In the
288 conditioning session, there was again evidence of increased startle responses to
289 shock (Figure 5C) in C*3*$^{-/-}$ mice and responses were of a similar magnitude in C*5*$^{-/-}$
290 mice, although these were not significantly different to wildtype. We replicated the
291 previous finding of enhanced fear-potentiated startle in *C3*$^{-/-}$ mice (Figure 5D), but

292 critically *C5*$^{-/-}$ mice showed no evidence of enhanced fear learning and were
293 comparable to wildtypes, indicating that loss of iC3b/CR3 signalling, but not loss of
294 C5a/C5aR and the terminal pathway, was involved in the *C3*$^{-/-}$ fear learning phenotype.
295 Additionally, we did not observe innate anxiety-like phenotypes in *C5*$^{-/-}$ mice (Figure
296 S5).
297
298 This pattern of effects allowed us to distinguish between the likely mechanisms
299 underlying the enhanced learned fear in *C3*$^{-/-}$ mice, as we could exclude concomitant
300 loss of C5a/C5aR signalling or molecules downstream of C5, and hence also exclude
301 an explanation based on effects of C5a/C5aR signalling on developmental
302 neurogenesis[51,52]. Instead, these data raised the possibility of an explanation based
303 on the established effects of the iC3b/CR3 pathway on synaptic pruning, a mechanism
304 involving microglia mediated elimination of synapses impacting on neurodevelopment
305 and learning-related synaptic plasticity[13,14,53].
306
307 **Differential expression of stress and anxiety related genes in *C3aR*$^{-/-}$ and *C3*$^{-/-}$**
308 **mice**
309 We next sought to assess whether the dissociations in innate anxiety and learned fear
310 between *C3aR*$^{-/-}$ and *C3*$^{-/-}$ models were associated with differential gene expression in
311 brain regions associated with emotional behaviours. We assayed gene expression in
312 three regions with known roles in stress and anxiety; the medial prefrontal cortex
313 (mPFC), ventral hippocampus (vHPC) and cerebellum[28,54](Figure 6A). Given our
314 previous data showing differential corticosterone responses and altered sensitivity to
315 diazepam in both knockouts, we first measured expression of the glucocorticoid
316 receptor *Nr3c1* and the corticotrophin-releasing hormone receptor 1 *Crhr1*, together
317 with *Gabra2* which encodes the $GABA_A$ receptor α2 subunit responsible for mediating

318 benzodiazepine anxiolysis[55]. There were no effects of genotype on *Crhr1* and *Gabra2*
319 mRNA expression in any of the brain regions assayed (Figure 6B,C). *Nr3c1*
320 expression did however show effects of genotype with strong trends indicating specific
321 increases in *C3aR*$^{-/-}$ mice in mPFC and vHPC and significantly increased expression
322 in cerebellum that was common to both knockouts (Figure 6D). As activation of C3aR
323 has been shown to stimulate calcium influx from the extracellular space[2-4,56,57] and
324 calcium channel subunit variants have strong links to risk for psychiatric and
325 neurological disorders, as well as anxiety phenotypes[58,59], we also investigated a
326 panel of voltage-gated calcium channels. Expression of *Cacna1d,* which encodes the
327 Cav1.3 channel of L-type calcium gated voltage channels, was increased in the mPFC
328 of *C3aR*$^{-/-}$ mice (Figure 6E) and in both *C3*$^{-/-}$ and *C3aR*$^{-/-}$ mice there was upregulation
329 of cerebellar *Cacna1e,* which encodes the Cav2.3 channel of R-type voltage gated
330 calcium channels (Figure 6F). We also investigated the expression of *Cacna1c* which
331 encodes the Ca_v1.2 subunit of L-type voltage gated calcium channels that forms the
332 channel pore allowing calcium entry[60]. We found genotype and brain region specific
333 changes in *Cacna1c* expression, with selective increases in expression in *C3aR*$^{-/-}$ mice
334 in the vHPC and cerebellum, but not the mPFC (Figure 6G).
335

336 **Discussion**

337 We have used knockout models manipulating specific complement proteins to reveal
338 dissociable effects of complement pathways on distinct elements of aversive
339 behaviours. A main finding was a profound innate anxiety phenotype in the *C3aR*$^{-/-}$
340 mice that was absent in *C3*$^{-/-}$ mice. The specificity of the anxiety phenotype exhibited
341 by *C3aR*$^{-/-}$ mice at the behavioural level was paralleled by EPM-evoked corticosterone
342 levels, confirming the validity of the EPM as an index of anxiety-like behaviour. A

343 second main finding was a double dissociation in terms of fear learning, whereby *C3*-
344 */-* and not *C3aR*$^{-/-}$ mice displayed enhanced conditioned fear reactivity. Using *C5*$^{-/-}$
345 mice, we concluded that the mechanisms accounting for the fear learning phenotype
346 in *C3*$^{-/-}$ mice are likely to arise from lack of iC3b/CR3 pathway activity. Although the
347 data presented here was in males, we can report that the same highly specific double
348 dissociation between innate anxiety and learned fear was also seen in females
349 (Supplementary Figures S6-9) extending the broader applicability of our findings.
350 These data indicate distinct effects mediated by closely related elements of the
351 complement system that differentially impact upon the neural mechanisms underlying
352 innate anxiety and learned fear.
353
354 Our use of specific complement knockout models allowed us to pinpoint the likely
355 complement pathways and potential mechanisms underlying the observed
356 phenotypes. Since C3a is solely produced via C3 cleavage, and C3aR is the canonical
357 receptor for C3a, we expected that any phenotypes dependent on the binding of C3a
358 to the C3aR would be apparent in both *C3*$^{-/-}$ and *C3aR*$^{-/-}$ models. However, this was
359 not borne out in our data. Given the divergence in innate anxiety phenotypes seen,
360 one explanation is that the *C3aR*$^{-/-}$ phenotypes are independent of C3a and instead
361 mediated by an alternative ligand. It has long been speculated that there may be
362 promiscuity of the C3aR due to its unusually large second extracellular loop[61]. Indeed,
363 a cleavage fragment of the neuropeptide precursor protein VGF (non-acronymic),
364 TLQP-21, was recently reported to bind the C3aR[62,63]. This peptide has pleiotropic
365 roles including in the stress response[64] and its precursor VGF is widely expressed
366 throughout the CNS[65] and in regions associated with stress reactivity and C3aR
367 expression such as the hypothalamus[66,67]. Determining whether the mechanisms

368 underlying innate anxiety phenotypes in *C3aR*$^{-/-}$ mice are dependent on TLQP-
369 21/C3aR interactions will be a priority for future work.
370
371 Whether the *C3aR*$^{-/-}$ phenotypes described here are the result of ongoing effects of
372 *C3aR* deletion in the adult brain or instead the enduring consequence of
373 neurodevelopmental impacts of *C3aR* deficiency also remains to be determined. On
374 the basis of previous findings implicating C3aR in both developmental neurogenesis[68]
375 and in acute brain changes following behavioural manipulations[69], both are
376 possibilities. One strategy would be to test whether acute administration of the C3aR
377 antagonist SB290157[70] phenocopies the constitutive knockout of *C3aR*, though at
378 present no data is available on the CNS penetration of SB290157 and this molecule
379 has received criticism due to evidence of agonist activity[71].
380
381 We also probed mechanisms underpinning the *C3aR*$^{-/-}$ innate anxiety phenotype by
382 assessing the effects of the anxiolytic drug diazepam. We found that a dose of
383 diazepam that was anxiolytic in wildtype mice had no effect in *C3aR*$^{-/-}$ mice. Stretch
384 attend postures, postulated to reflect risk assessment behaviour[46], are highly sensitive
385 to pharmacological manipulation[40,72] and in agreement with our own findings,
386 diazepam has been shown to specifically decrease SAPs in the absence of effects on
387 open arm exploration[73]. Importantly, *C3aR*$^{-/-}$ mice consistently performed more SAPs
388 than other genotypes, and therefore floor effects cannot account for the pattern of
389 results observed. Benzodiazepines act on $GABA_A$ receptors[55] however we found no
390 significant changes in expression of *Gabra2*, a $GABA_A$ receptor subunit responsible
391 for anxiolytic actions of benzodiazepines in tests of innate anxiety[55], in the brain
392 regions sampled. This raises the possibility of alternative molecular mechanisms

393 mediating the anxiety phenotypes seen in the *C3aR*$^{-/-}$ model. Whatever the molecular
394 underpinnings of the dissociable anxiety phenotypes, our data show a profoundly
395 altered effect of diazepam in both knockouts; a lack of response in *C3aR*$^{-/-}$ and an
396 apparent paradoxical anxiogenic effect of the drug in *C3*$^{-/-}$ mice, though this
397 interpretation needs to take into account an apparent selective sedative effect in *C3*$^{-/-}$
398 mice.
399
400 In contrast to innate anxiety, we observed a specific effect of *C3* knockout on
401 conditioned fear. The absence of a comparable phenotype in *C3aR*$^{-/-}$ and *C5*$^{-/-}$ mice
402 suggested that these effects were unlikely to be due to loss of either C3a/C3aR,
403 C5a/C5aR, or the terminal pathway, and instead that enhanced fear learning
404 phenotypes in *C3*$^{-/-}$ mice were likely dependent on loss of the iC3b/CR3 pathway. This
405 pathway has been strongly implicated in activity dependent synaptic elimination during
406 neurodevelopment[13,25] and in age-dependent synapse loss[74]. While demonstrations
407 of complement mediated synaptic pruning during development have centered on the
408 visual system, complement-mediated microglial phagocytosis of dopamine D1
409 receptors has been demonstrated in the nucleus accumbens with functional impacts
410 on social behaviour[75]. It remains to be seen whether complement mediated processes
411 of this nature, within brain regions linked to fear processing such as the ventral
412 hippocampus, amygdala and prefrontal cortex are responsible for enhanced fear
413 learning in *C3*$^{-/-}$ mice, or whether this phenotype is a general consequence of altered
414 synaptic elimination throughout the *C3*$^{-/-}$ brain. In addition to developmental processes,
415 the iC3b/CR3 pathway could also be involved acutely in fear learning. *C3* mRNA is
416 upregulated during discrete stages of fear learning[69] and microglial CR3 is implicated

417 in long term depression[76]. Furthermore, complement-mediated engulfment of
418 synapses by microglia may be important in the forgetting of fear memories[14].
419
420 At the gene expression level, we found some changes which were common to both
421 knockouts, and one result that was specific to *C3aR*$^{-/-}$ mice. Regarding the latter, there
422 was a highly specific increase in expression of *Cacna1c* in the ventral hippocampus
423 and cerebellum of *C3aR*$^{-/-}$ mice. This finding is of potential interest given the strong
424 evidence implicating *CACNA1C* variants in genetic risk for a broad spectrum of
425 psychiatric disorders including schizophrenia and bipolar disorder[58], with anxiety
426 phenotypes reported in both human risk variant carriers[77] and animal models[78-81].
427 Whether alterations in *Cacna1c* are of functional relevance to the *C3aR*$^{-/-}$ anxiety
428 phenotypes observed here remains to be determined. We also observed increased
429 cerebellar expression of the glucocorticoid receptor in both *C3*$^{-/-}$ and *C3aR*$^{-/-}$ mice,
430 suggesting that these alterations may result from the absence of C3a/C3aR signalling.
431 Expression of these genes did not differentiate between models and therefore were
432 unlikely to contribute to the dissociable effects of the knockouts on behaviour and
433 stress hormone physiology. Neuronal activity in the ventral hippocampus as indexed
434 by *c-Fos* gene expression after exposure to the EPM also failed to differentiate
435 between genotypes, and hence activity in other brain regions in particular the
436 amygdala and hypothalamus may be more informative in terms of functional
437 neuroanatomy underlying the anxiety-related behavioural and physiological
438 differences seen in the knockout models.
439
440 Anxiety and fear are commonly comorbid with depression and recent preclinical work
441 has suggested a protective role for C3a/C3aR in chronic-stress induced depressive-

442 behaviour[82]. Given the common co-occurrence of anxiety and depression, our findings
443 of enhanced anxiety in *C3aR*$^{-/-}$ mice might seem at odds with the reported resilience
444 of this strain[-] to depression-related phenotypes[82]. However, the chronic unpredictable-
445 stress paradigm used in these studies is likely to evoke significant inflammation, and
446 therefore the extent to which our data in acutely stressed animals can be compared is
447 questionable. In summary, our findings add significantly to the evidence that
448 perturbations of the complement system, whether reduced complement activation as
449 in the present work or excessive activation as is predicted by *C4* genetic variants[24,83],
450 have major and dissociable effects on brain and behavioural phenotypes of relevance
451 to core clinical symptoms of psychiatric disease.
452

453 **Materials and Methods**

454 **Mouse models and husbandry.** Wildtype and *C3*$^{-/-}$ strains were sourced in-house
455 from Professor B. Paul Morgan and Dr Timothy Hughes (strains originally from The
456 Jackson Laboratory; B6.PL-Thy1^{a}/CyJ stock#000406 and B6;129S4-C3tm1Crr/J
457 stock#003641 respectively); *C3aR*$^{-/-}$ mice were provided by Professor Craig Gerard of
458 Boston Children's Hospital, USA (strain originally from The Jackson Laboratory, strain
459 C.129S4-C3ar1^{tm1Cge}/J, stock#005712, subsequently backcrossed to C57Bl/6J).
460 *C5*$^{-/-}$ mice (as described in [84]) were kindly donated by Professor Marina Botto, Imperial
461 College London. This strain originated from naturally C5-deficient DBA/2J mice, that
462 had been backcrossed to C57Bl/6J. *C3*$^{-/-}$, *C3aR*$^{-/-}$ and *C5*$^{-/-}$ strains were maintained via
463 homozygous breeding on a C57Bl/6J background and in all experiments were
464 compared to wildtype mice also on a C57Bl/6J background. Male mice (3-8 months
465 old during experimental testing) were kept in a temperature and humidity-controlled
466 vivarium (21±2°C and 50±10%, respectively) with a 12-hour light-dark cycle (lights on

467 at 07:00hrs/lights off at 19:00hrs). Home cages were environmentally enriched with
468 cardboard tubes, soft wood blocks and nesting materials and animals were housed in
469 single sex littermate groups (2-5 mice/cage). Standard laboratory chow and water
470 were available *ad libitum*. All procedures were performed in accordance with the
471 requirements of the UK Animals (Scientific Procedures) Act (1986).
472
473 **General behavioural methods.** Testing took place between the hours of 09:00 and
474 17:00, with random distribution of testing for subjects of different genotypes throughout
475 the day. Mice were habituated to the test rooms for 30 min prior to testing. All assays
476 involved individual testing of mice and apparatus was cleaned thoroughly with a 70%
477 ethanol solution between subjects.
478
479 **Data collection.** Data for the EPM, EZM and Open Field were collected using
480 EthoVision XT software (Noldus Information Technology, Netherlands) via a video
481 camera mounted above the centre of each piece of apparatus. Tracking of each
482 subject was determined as the location of the greater body-proportion (12 frames/s) in
483 the specific virtual zones of each piece of apparatus.
484
485 **The elevated plus maze (EPM).** The maze, positioned 300 mm above the floor and
486 illuminated evenly at 15 lux, was constructed of opaque white Perspex and consisted
487 of two exposed open arms (175 x 78 mm^2, length x width, no ledges) and two equally
488 sized enclosed arms, which had 150 mm high walls [85]. Equivalent arms were arranged
489 opposite one another. Subjects were placed at the enclosed end of a closed arm and
490 allowed to freely explore for 5 minutes. Data from each pair of arms were combined
491 to generate single open and closed arm values (number and duration of arm entries

492 and latency of first entry to each arm). In addition, the following parameters were
493 manually scored (by an experimenter positioned at a computer in the same room as
494 the maze, watching the live-video stream of the test); number of stretch-attend
495 postures (SAPs; defined as the animal slowly and carefully reaching towards the open
496 arms in a low, elongated body posture[86,87]) and number of head dips from the open
497 arms (looking down over the edge of an open arm).
498
499 **The elevated zero maze (EZM).** The maze, positioned 520 mm above the floor and
500 illuminated evenly at 15 lux, was constructed of wood and consisted of two exposed
501 open regions (without ledges; 52 mm wide) and two equally sized enclosed regions
502 (also 52 mm wide), which had 200 mm high grey opaque walls. The diameter of the
503 maze was 600mm. Equivalent regions were arranged opposite one another. Subjects
504 were placed at the border of one of the open and closed regions and allowed to freely
505 explore for 5 min. Data from each pair of regions were combined to generate single
506 open and closed region values (number and duration of region entries and latency of
507 first entry to each region). In addition, the number of head dips (as above) were
508 measured. Due to the high walls of the enclosed sections of the maze, subjects were
509 not visible to the experimenter when in the closed regions and therefore these
510 parameters were scored only when a subject was on the open regions.
511
512 **Locomotor activity (LMA).** LMA was measured in an apparatus consisting of twelve
513 transparent Perspex chambers (each 210 x 360 x 200 mm, width x length x height).
514 Two infrared beams were embedded within the walls of each chamber, which crossed
515 the chamber 30 mm from each end and 10 mm from the chamber floor. Individual
516 subjects were placed in a designated chamber for a 120 min duration on three

517 consecutive days. Beam breaks were recorded as an index of activity, using a
518 computer running custom written BBC Basic V6 programme with additional interfacing
519 by ARACHNID (Cambridge Cognition Ltd, Cambridge, UK). Data were analysed as
520 the total number of beam breaks per session per day.
521
522 **Fear-potentiated startle (FPS).** FPS was assessed using startle chamber apparatus
523 which consisted of a pair of ventilated and soundproofed SR-LAB startle chambers
524 (San Diego Instruments, CA, USA) each containing a non-restrictive Plexiglas cylinder
525 (35 mm in diameter), mounted on a Perspex plinth, into which a subject was placed.
526 The motor responses of subjects to white noise stimuli (generated from a speaker 120
527 mm above the cylinder) were recorded via a piezoelectric accelerometer, attached
528 centrally below the Plexiglas cylinder, which converted flexion plinth vibration into
529 electrical signals. The peak startle response, within 200ms from the onset of each
530 startle presentation, in each trial, was normalized for body weight differences using
531 Kleiber's 0.75 mass exponent[88] as per[85]. A computer running SR-Lab software
532 (Version 94.1.7.48) was used to programme trials and record data. A foot shock grid
533 connected to a shock generator (San Diego Instruments, CA, USA) was inserted into
534 the Plexiglas cylinder before conditioning sessions.
535
536 FPS consisted of three separate sessions presented over a two-day period (see Figure
537 4A). On the first day, mice were given a pre-conditioning session immediately followed
538 by the conditioning session. The pre-conditioning session started with a 5 min
539 acclimatisation phase followed by presentation of 3 no-stimulus trials, and then a block
540 of pulse-alone trials presented at 90, 100 and 110dB (5 of each at 40 ms duration).
541 Trials were randomly distributed throughout the session and presented with a 60 s

542 random interval (range 36 s to 88 s). After the pre-conditioning session was complete,
543 mice were removed from the startle chambers, restraint tubes cleaned, and shock
544 grids were placed into the Plexiglas cylinders prior to commencing the conditioning
545 session. The mice were then returned to the startle chambers and subjected to a
546 session consisting of a 5 min acclimatisation phase followed by 3 CS+shock trials, with
547 3 no stimulus trials before and after, presented with a 2min random interval (range 1.5
548 to 3min). The scrambled 0.14 mA, 0.5 s foot shock was delivered in the final 0.5 s of
549 the 30 s visual CS. Following a 24hr delay, subjects were assessed for FPS in the
550 post-conditioning session. This session followed the same format as the pre-
551 conditioning session (5 min acclimatisation phase followed by presentation of 3 no-
552 stimulus trials, and then a block of pulse-alone trials presented at 90, 100 and 110dB,
553 with 5 of each at 40 ms duration) however the final block of trials also included
554 pulse+CS trials at 90, 100 and 110 dB (5 of each), with the startle pulse presented in
555 the final 40 ms of the CS. FPS was determined as the fold change between pulse-
556 alone trials and pulse+CS trials within the post-conditioning session.
557
558 **Corticosterone measurements.** Testing took place between the hours of 10:00 and
559 14:00 to account for the diurnal pattern of corticosterone release[89]. Mice were allowed
560 to freely explore the EPM for 5 min, after which they were placed in a holding cage for
561 a further 25 min before being culled by cervical dislocation. Control mice were
562 removed from their home cage and immediately culled. There was an equal
563 distribution of subjects of different genotypes, counterbalanced between the two test
564 conditions and throughout the testing period. Trunk blood was collected into heparin
565 tubes (Becton Dickinson, USA) and immediately centrifuged at 4000 rpm for 10 min,
566 and the supernatant removed and frozen at -80°c until further use. A corticosterone

567 ELISA was performed according to manufacturer's instructions (ADI-900-097, Enzo
568 Life Sciences, UK) and analysed using a four-parameter logistic curve plug in
569 (https://www.myassays.com/four-parameter-logistic-curve.assay).
570
571 **Immediate early gene (IEG) experiment.** Mice were allowed to freely explore the
572 EPM for 5 min, after which they were placed in a holding cage for a further 25 min
573 before being culled by cervical dislocation. Control mice were removed from their
574 home cage and immediately culled. Brains were removed and the ventral
575 hippocampus (vHPC; the whole hippocampus was dissected and the posterior third
576 was collected) was dissected and frozen at -80° until further use. Tissue was
577 processed for qPCR analyses as detailed below.
578
579 ***Diazepam study.*** Wildtype, *C3*$^{-/-}$ and *C3aR*$^{-/-}$ were used and were randomly assigned
580 to either vehicle or drug conditions within each genotype. A three-day dosing regimen
581 of diazepam (2 mg/kg, i.p., Hameln Pharmaceuticals, UK) or an equivalent volume of
582 vehicle (0.1 M phosphate buffered saline, pH 7.4) was used. Following 2 days of pre-
583 treatment, diazepam or vehicle was administered 30 min prior to testing on the EPM
584 on the 3rd day.
585
586 **Tissue for gene expression analysis.** Mice were removed from their home cage and
587 immediately culled via cervical dislocation. Brains were removed from mice in both
588 conditions, and the following regions dissected: medial prefrontal cortex (mPFC),
589 ventral hippocampus (vHPC) and cerebellum (see Figure 6A) and frozen at -80° until
590 further use.
591

592 **Quantitative Polymerase Chain Reaction (qPCR).** Gene expression was analysed
593 using standardised qPCR methods with quantification using the $2^{-\Delta\Delta Ct}$ method[90].
594 Mouse brain tissue from the mPFC, vHPC and the cerebellum was analysed. RNA
595 was extracted using the RNeasy kit (QIAGEN) and was subsequently treated with
596 DNAse to remove genomic DNA (TURBO DNA-free kit, Thermo Fisher Scientific).
597 RNA was then converted to cDNA (RNA to cDNA EcoDry Premix, Random Hexamers,
598 Clontech, Takara). cDNA samples were run in triplicate in 96 well reaction plates using
599 SYBR-Green-based qPCR (SensiFast, HI-ROX, Bioline) according to manufacturer's
600 instructions using a StepOnePlus System (Applied Biosystems, Thermo Fisher
601 Scientific). Genotypes were counterbalanced across plates and genes of interest were
602 run alongside housekeeping genes *Gapdh* and *Hrpt1* for each sample, within the same
603 reaction plate. All samples were run in triplicate and samples differing by >0.3 Cts
604 were excluded. The change in expression of genes of interest, after normalisation to
605 the two house-keeping genes (ΔCt) was transformed to yield $2^{-\Delta\Delta Ct}$ values. Relative
606 changes from wildtype animals were calculated for each gene of interest.
607
608 ***Primers***
609 Primers were designed to span at least one exon-exon junction and to match the target
610 sequence only in mouse (Primer-Blast, NCBI) and were synthesised commercially
611 (Sigma Aldrich). Primer efficiency was determined separately through a dilution series
612 of cDNA samples from wildtype hippocampus, cerebellum and cortex. Primers with an
613 efficiency between 90-110% were selected.
614
615
616

617 **Table 1**. List of primer sequences used.

Gene	Species	Forward	Reverse
Gapdh	Mouse	GAACATCATCCCTGCATCCA	CCAGTGAGCTTCCCGTTCA
Hprt1	Mouse	TTGCTCGAGATGTCATGAAGGA	AATGTAATCCAGCAGGTCAGCAA
Gabra2	Mouse	AAGCCACTGGAGGAAAACATCT	TTAGCCAGCACCAACCTGAC
Crhr1	Mouse	CTTCAACTCTTTCCTGGAGTCCT	TGGCAGAGCGGACCTCA
Nr3c1	Mouse	AAACTCTGCCTGGTGTGCTC	GGTAATTGTGCTGTCCTTCCAC
Cacna1c	Mouse	ATGGTTCTTGTCAGCATGTTGCGG	TGCAAATGTGGAACCGGTAAGTG
Cacna1d	Mouse	AGAGGACCATGCGAACGAG	CCTTCACCAGAAATAGGGAGTCT
Cacna1e	Mouse	CTCATGTCACCACCGCTAGG	TCTGTCTGCACCACCTTTGG
cFos	Mouse	CTCCAAGCGGAGACAGATCAA	TCGGTGGGCTGCCAAAATAA
Zif268	Mouse	GACCACAGAGTCCTTTTCTGACA	CTGAAAAGGGGTTCAGGCCA

618

619 **Genotyping** Genotyping was performed on post-mortem tail tip samples. Qiagen
620 DNeasy Blood and Tissue Kits (Qiagen, Manchester, UK) were used to extract
621 genomic DNA (gDNA) as per the manufacturers standard protocol. For *C3*$^{-/-}$ mice, JAX
622 protocol 27746 was used (common; ATCTTGAGTGCACCAAGCC, wildtype;
623 GGTTGCAGCAGTCTATGAAGG, mutant; GCCAGAGGCCACTTGTATAG) and for
624 *C3aR*$^{-/-}$ JAX protocol 27638 was used (common; AGCCATTCTAGGGGCGTATT, wild
625 type reverse; CATGGTTTGGGGTTATTTCG, mutant reverse;
626 TTGATGTGGAATGTGTGCGAG). For both genotypes, a touchdown cycling protocol
627 was used (see JAX protocols for details). Genotyping for *C5*$^{-/-}$ mice was performed as
628 described in [84].

629

630 **Statistical analysis.** All statistical analyses were carried out using GraphPad Prism
631 8.4.1 (GraphPad Software, CA, USA). Data was assessed for equality of variances

632 using the Brown-Forsythe test and then appropriate parametric (*t* test, one-way or two-
633 way ANOVA) or non-parametric (Kruskal-Wallis) tests used. *Post hoc* pairwise
634 comparisons were performed using the Tukey or Dunn's tests for parametric or non-
635 parametric analyses, respectively. For all analyses, alpha was set to 0.05 and exact p
636 values were reported unless $p<0.0001$. All p values were multiplicity adjusted[91]. Data
637 are expressed as mean ± standard error of the mean.
638
639 The main between-subjects' factor for all ANOVA analyses was GENOTYPE (WT, *C3*$^{-}$
640 $^{/-}$, *C3aR*$^{-/-}$, or *C5*$^{-/-}$). For the EPM, LMA and FPS experiments, there were within-
641 subject factors of ZONE (open, closed, middle), DAY (1,2,3) and STIMULUS
642 INTENSITY (90, 100, 110 dB) respectively. Analysis of plasma corticosterone by two-
643 way ANOVA included an additional between subject factor of CONDITION (baseline,
644 EPM), and for the diazepam experiment, there was an additional between subject
645 factor of DRUG (diazepam, vehicle). For qPCR analyses, ΔCt values were analysed
646 by one-way ANOVA.
647
648
649
650
651
652
653
654
655
656

657 **Author's contributions**

658 The study was designed by LJW, TH, BPM, WPG and LSW. LJW and TH performed
659 behavioural experiments with assistance from NH. Molecular analyses were
660 performed by SAB, EB, MT, ALM, SAB, EB, MT, NL, AIB and LJW. Data interpretation
661 were carried out by JH, MJO, JR, WPG, NH, TRH, BPM, LSW and TH. The manuscript
662 was drafted by LJW, TH, WPG and LSW. All authors approved the final manuscript.

663

664 **Acknowledgements**

665 The authors thank Professor Craig Gerard and Professor Marina Botto for provision of
666 the *C3aR*$^{-/-}$ and *C5*$^{-/-}$ strains respectively, and to Rhys Perry, Pat Mason, Helen Read
667 and other staff at JBIOS for their invaluable animal care and husbandry. Thanks also
668 to Dr Emma Watts for her feedback on the manuscript. This work was supported by a
669 Wellcome Trust Integrative Neuroscience PhD Studentship awarded to LJW
670 (099816/Z/12/Z), a Waterloo Foundation Early Career Fellowship awarded to LJW, a
671 Hodge Centre for Neuropsychiatric Immunology Seed Corn and Project grant awarded
672 to LJW and a Wellcome Trust Strategic Award 100202/Z/12/Z (DEFINE) held by the
673 Neuroscience and Mental Health Research Institute at Cardiff University.

674

675 **Competing financial interests**

676 The authors declare no competing financial interests.

677

678 **Materials and correspondence**

679 All data from this study are available from the corresponding authors upon reasonable
680 request.

681

682 **References**

683

684 1. Coulthard, L. G. & Woodruff, T. M. Is the Complement Activation Product
685 C3a a Proinflammatory Molecule? Re-evaluating the Evidence and the
686 Myth. *J. Immunol.* **194,** 3542–3548 (2015).
687 2. Norgauer, J. *et al.* Complement fragment C3a stimulates Ca2+ influx in
688 neutrophils via a pertussis-toxin-sensitive G protein. *Eur. J. Biochem.*
689 **217,** 289–294 (1993).
690 3. Möller, T., Nolte, C., Burger, R., Verkhratsky, A. & Kettenmann, H.
691 Mechanisms of C5a and C3a Complement Fragment-Induced [Ca2+]i
692 Signalling in Mouse Microglia. *Journal of Neuroscience* **17,** 615–624
693 (1997).
694 4. Lian, H., Li, Y., Lu, H.-C. & Zheng, H. NFκB-Activated Astroglial Release
695 of Complement C3 Compromises Neuronal Morphology and Function
696 Associated with Alzheimer's Disease. *Neuron*, **85,** 101–115 (2015).
697 5. Sayah, S. *et al.* Two different transduction pathways are activated by C3a
698 and C5a anaphylatoxins on astrocytes. *Molecular Brain Research* **112,**
699 53–60 (2003).
700 6. Morley, B. J. & Walport, M. J. *The Complement FactsBook*. (Academic
701 Press, 1999).
702 7. Kemper, C. & Köhl, J. Back to the future – non-canonical functions of
703 complement. *Seminars in Immunology* **37,** 1–3 (2018).
704 8. Nataf, S., Stahel, P. F., Davoust, N. & Barnum, S. R. Complement
705 anaphylatoxin receptors on neurons: new tricks for old receptors? *Trends*
706 *Neurosci.* **22,** 397–402 (1999).
707 9. Veerhuis, R., Nielsen, H. M. & Tenner, A. J. Complement in the brain.
708 *Molecular Immunology* **48,** 1592–1603 (2011).
709 10. Bénard, M., Gonzalez, B. J., Biological, M. S. J. O.2004. Characterization
710 of C3a and C5a receptors in rat cerebellar granule neurons during
711 maturation neuroprotective effect of C5a against apoptotic cell death. *J*
712 *Biol. Chem,* **42***,* 43487-43496 (2004).
713 11. Rahpeymai, Y. *et al.* Complement: a novel factor in basal and ischemia-
714 induced neurogenesis. *EMBO J* **25,** 1364–1374 (2006).
715 12. Gorelik, A. *et al.* Developmental activities of the complement pathway in
716 migrating neurons. *Nature Communications* **8,** 15096 (2017).
717 13. Stevens, B. *et al.* The classical complement cascade mediates CNS
718 synapse elimination. *Cell* **131,** 1164–1178 (2007).
719 14. Wang, C. *et al.* Microglia mediate forgetting via complement-dependent
720 synaptic elimination. *Science,* **367,** 688-694 (2020).
721 15. Harold, D. *et al.* Genome-wide association study identifies variants at
722 CLU and PICALM associated with Alzheimer's disease. *Nature Genetics*
723 **41,** 1088–1093 (2009).
724 16. Jansen, I. E. *et al.* Genome-wide meta-analysis identifies new loci and
725 functional pathways influencing Alzheimer's disease risk. *Nature Genetics*
726 **51**, 404–413 (2019).
727 17. Shi, Q. *et al.* Complement C3-Deficient Mice Fail to Display Age-Related
728 Hippocampal Decline. *Journal of Neuroscience* **35,** 13029–13042 (2015).

18. Zhou, J., Fonseca, M. I., Pisalyaput, K. & Tenner, A. J. Complement C3 and C4 expression in C1q sufficient and deficient mouse models of Alzheimer's disease. *Journal of Neurochemistry* **106,** 2080–2092 (2008).
19. Corbett, B. A. *et al.* A proteomic study of serum from children with autism showing differential expression of apolipoproteins and complement proteins. *Mol. Psychiatry* **12,** 292 (2007).
20. Maes, M., Delange, J., Ranjan, R., Meltzer, H. Y. & Desnyer, R. Acute phase proteins in schizophrenia, mania and major depression: modulation by psychotropic drugs. *Psychiatry Research,* **66,** 1–11 (1997).
21. Ruland, T. *et al.* Molecular serum signature of treatment resistant depression. *Psychopharmacology* 1–9 (2016).
22. Song, Y. R. *et al.* Specific alterations in plasma proteins during depressed, manic, and euthymic states of bipolar disorder. *Brazilian Journal of Medical and Biological Research* **48,** 973–982, (2015).
23. Oganesyan, L. P., Mkrtchyan, G. M., Sukiasyan, S. H. & Boyajyan, A. S. Classic and alternative complement cascades in post-traumatic stress disorder. *Bull. Exp. Biol. Med.* **148,** 859–861 (2009).
24. Sekar, A. *et al.* Schizophrenia risk from complex variation of complement component 4. *Nature,* ***530,*** 117–183 (2016).
25. Schafer, D. P. *et al.* Microglia Sculpt Postnatal Neural Circuits in an Activity and Complement-Dependent Manner. *Neuron* **74,** 691–705 (2012).
26. Håvik, B. *et al.* The Complement Control-Related Genes CSMD1 and CSMD2 Associate to Schizophrenia. *BPS* **70,** 35–42 (2011).
27. Zhang, S. *et al.* Association Between Polymorphisms of the Complement 3 Gene and Schizophrenia in a Han Chinese Population. *Cell. Physiol. Biochem.* **46,** 2480–2486 (2018).
28. Tovote, P., Fadok, J. P. & Lüthi, A. Neuronal circuits for fear and anxiety. *Nat. Rev.* **16,** 317–331 (2015).
29. Perusini, J. N. & Fanselow, M. S. Neurobehavioral perspectives on the distinction between fear and anxiety. *Learn. Mem.* **22,** 417–425 (2015).
30. Davis, M. Neural systems involved in fear and anxiety measured with fear-potentiated startle. *Am Psychol* **61,** 741–756 (2006).
31. Engin, E. *et al.* Modulation of anxiety and fear via distinct intrahippocampal circuits. *eLife,* **5:e14120**, (2016).
32. Vogelzangs, N., Beekman, A. T. F., de Jonge, P. & Penninx, B. W. J. H. Anxiety disorders and inflammation in a large adult cohort. *Translational Psychiatry* **3,** e249–e249 (2013).
33. Girardi, G. *et al.* Imaging of activated complement using ultrasmall superparamagnetic iron oxide particles (USPIO)-conjugated vectors: An in vivo in utero non-invasive method to predict placental insufficiency and abnormal fetal brain development. *Mol. Psychiatry* **20,** 1017–1026 (2015).
34. Kulkarni, A. P., Govender, D. A., Kotwal, G. J. & Kellaway, L. A. Modulation of anxiety behavior by intranasally administered Vaccinia virus complement control protein and curcumin in a mouse model of Alzheimer's disease. *Current Alzheimer Research* **8,** 95–113 (2011).
35. Fischer, M. B., Ma, M., Goerg, S., Zhou, X. & Xia, J. Regulation of the B cell response to T-dependent antigens by classical pathway complement. *J.Immunol,* **157,** 549-556, (1996).

36. Humbles, A. A. *et al*. A role for the C3a anaphylatoxin receptor in the effector phase of asthma. *Nature,* **406,** 998–1001 (2000).
37. Pellow, S., Chopin, P., File, S. E. & Briley, M. Validation of open : closed arm entries in an elevated plus-maze as a measure of anxiety in the rat. *J. Neurosci. Methods* **14,** 149–167 (1985).
38. Walf, A. A. & Frye, C. A. The use of the elevated plus maze as an assay of anxiety-related behavior in rodents. *Nat Protoc* **2,** 322–328 (2007).
39. Ennaceur, A. Tests of unconditioned anxiety - pitfalls and disappointments. *Physiology & Behavior* **135,** 55–71 (2014).
40. RODGERS, R. J. Anxiety, defence and the elevated plus-maze. *Neuroscience and Biobehavioural Reviews,* **21,** 801-810, (1997).
41. Braun, A. A., Skelton, M. R., Vorhees, C. V. & Williams, M. T. Comparison of the elevated plus and elevated zero mazes in treated and untreated male Sprague-Dawley rats: Effects of anxiolytic and anxiogenic agents. *Pharmacology Biochemistry and Behavior* **97,** 406–415 (2011).
42. Kheirbek, M. A. *et al.* Differential Control of Learning and Anxiety along the Dorsoventral Axis of the Dentate Gyrus. *Neuron* **77,** 955–968 (2013).
43. Kubik, S., Miyashita, T. & Guzowski, J. F. Using immediate-early genes to map hippocampal subregional functions. *Learning & Memory* **14,** 758–770 (2007).
44. Lepicard, E. M., Joubert, C., Hagneau, I., Perez-Diaz, F. & Chapouthier, G. Differences in anxiety-related behavior and response to diazepam in BALB/cByJ and C57BL/6J strains of mice. *Pharmacology Biochemistry and Behavior* **67,** 739–748 (2000).
45. Grewal, S. S., SHEPHERD, J. K., Bill, D. J., Fletcher, A. & Dourish, C. T. Behavioural and pharmacological characterisation of the canopy stretched attend posture test as a model of anxiety in mice and rats. *Psychopharmacology* **133,** 29–38, (1997).
46. Kaesermann, H. P. Stretched attend posture, a non-social form of ambivalence, is sensitive to a conflict-reducing drug action. *Psychopharmacology* **89,** 31–37, (1986).
47. Albrechet-Souza, L., Cristina de Carvalho, M., Rodrigues Franci, C. & Brandão, M. L. Increases in plasma corticosterone and stretched-attend postures in rats naive and previously exposed to the elevated plus-maze are sensitive to the anxiolytic-like effects of midazolam. *Hormones and Behavior* **52,** 267–273 (2007).
48. Holt, D. J., Coombs, G., Zeidan, M. A., Goff, D. C. & Milad, M. R. Failure of neural responses to safety cues in schizophrenia. *Arch Gen Psychiatry* **69,** 893–903 (2012).
49. Grillon, C., Morgan, C. A., Southwick, S. M., Davis, M. & Charney, D. S. Baseline startle amplitude and prepulse inhibition in Vietnam veterans with posttraumatic stress disorder. *Psychiatry Research* **64,** 169–178 (1996).
50. Falls, W. A., Carlson, S., Turner, J. G. & Willott, J. F. Fear-potentiated startle in two strains of inbred mice. *Behavioral Neuroscience* **111,** 855–861 (1997).
51. Coulthard, L. G. *et al.* Complement C5aR1 Signalling Promotes Polarization and Proliferation of Embryonic Neural Progenitor Cells through PKCζ. *J. Neurosci.* **37,** 5395–5407 (2017).

52. Hawksworth, O. A., Coulthard, L. G., Taylor, S. M., Wolvetang, E. J. & Woodruff, T. M. Brief Report: Complement C5a Promotes Human Embryonic Stem Cell Pluripotency in the Absence of FGF2. *Stem Cells,* **32,** 3278-3284, (2014).
53. Schafer, D. P. *et al.* Microglia sculpt postnatal neural circuits in an activity and complement-dependent manner. *Neuron* **74,** 691–705 (2012).
54. Apps, R. & Strata, P. Neuronal circuits for fear and anxiety - the missing link. *Nat. Rev.* **16,** 642 (2015).
55. Smith, K. S., Engin, E., Meloni, E. G. & Rudolph, U. Benzodiazepine-induced anxiolysis and reduction of conditioned fear are mediated by distinct GABAA receptor subtypes in mice. *Neuropharmacology* **63,** 250–258 (2012).
56. Ahamed, J., Venkatesha, R. T., Thangam, E. B. & Ali, H. C3a Enhances Nerve Growth Factor-Induced NFAT Activation and Chemokine Production in a Human Mast Cell Line, HMC-1. *J. Immunol.* **172,** 6961–6968 (2004).
57. Wu, F. *et al.* Complement component C3a plays a critical role in endothelial activation and leukocyte recruitment into the brain. *J Neuroinflammation* **13,** 23 (2016).
58. Hamshere, M. L. *et al.* Genome-wide significant associations in schizophrenia to ITIH3/4, CACNA1C and SDCCAG8, and extensive replication of associations reported by the Schizophrenia PGC. *Mol. Psychiatry* **18,** 708-712, (2019).
59. Kabir, Z. D. *et al.* Rescue of impaired sociability and anxiety-like behavior in adult *cacna1c*-deficient mice by pharmacologically targeting eIF2α. *Mol. Psychiatry* **22,** 1096–1109 (2017).
60. Simms, B. A. & Zamponi, G. W. Neuronal Voltage-Gated Calcium Channels: Structure, Function, and Dysfunction. *Neuron* **82,** 24–45 (2014).
61. Chao, T. H. *et al.* Role of the second extracellular loop of human C3a receptor in agonist binding and receptor function. *Journal of Biological Chemistry* **274,** 9721–9728 (1999).
62. Hannedouche, S. *et al.* Identification of the C3a Receptor (C3AR1) as the Target of the VGF-derived Peptide TLQP-21 in Rodent Cells. *Journal of Biological Chemistry* **288,** 27434–27443 (2013).
63. Cero, C. *et al.* The TLQP-21 peptide activates the G-protein-coupled receptor C3aR1 via a folding-upon-binding mechanism. *Structure* **22,** 1744–1753 (2014).
64. Razzoli, M. *et al.* Implication of the VGF-derived peptide TLQP-21 in mouse acute and chronic stress responses. *Behav. Brain Res.* **229,** 333–339 (2012).
65. van den Pol, A. N., Bina, K., Decavel, C. & Ghosh, P. VGF expression in the brain. *J. Comp. Neurol.* **347,** 455–469 (1994).
66. Lewis, B., Francis, K., Gasque, P., Scanlon, M. & Ham, J. Functional complement C3a receptors in the rat pituitary gland. *Endocrine Abstracts* **3,** 198 (2002).
67. Francis, K. Complement C3a receptors in the pituitary gland: a novel pathway by which an innate immune molecule releases hormones involved in the control of inflammation. *The FASEB Journal,* **17,** 2266-2268 (2003).

68. Coulthard, L. G., Hawksworth, O. A. & Woodruff, T. M. Complement: The Emerging Architect of the Developing Brain. *Trends Neurosci.* **41,** 373–384 (2018).
69. Scholz, B. *et al.* The Regulation of Cytokine Networks in Hippocampal CA1 Differentiates Extinction from Those Required for the Maintenance of Contextual Fear Memory after Recall. *PLoS ONE* **11,** e0153102–29 (2016).
70. Ames, R. S. *et al.* Identification of a selective nonpeptide antagonist of the anaphylatoxin C3a receptor that demonstrates antiinflammatory activity in animal models. *J. Immunol.* **166,** 6341–6348 (2001).
71. Therien, A. G., Baelder, R. & Köhl, J. Agonist Activity of the Small Molecule C3aR Ligand SB 290157. *J. Immunol.* **174,** 7479–7480 (2005).
72. Holly, K. S., Orndorff, C. O. & Murray, T. A. MATSAP: An automated analysis of stretch-attend posture in rodent behavioral experiments. *Scientific Reports* **6,** (2016).
73. Genewsky, A. *et al.* How much fear is in anxiety? Preprint at https://doi:10.1101/385823 (2018).
74. Hong, S. *et al.* Complement and microglia mediate early synapse loss in Alzheimer mouse models. *Science* **352,** 712–716 (2016).
75. Kopec, A. M., Smith, C. J., Ayre, N. R., Sweat, S. C. & Bilbo, S. D. Microglial dopamine receptor elimination defines sex-specific nucleus accumbens development and social behavior in adolescent rats. *Nature Communications* **9,** 3769 (2018).
76. Zhang, J. *et al.* Microglial CR3 Activation Triggers Long-Term Synaptic Depression in the Hippocampus via NADPH Oxidase. *Neuron* **82,** 195–207 (2014).
77. Roussos, P., Giakoumaki, S. G., Georgakopoulos, A., Robakis, N. K. & Bitsios, P. The CACNA1C and ANK3 risk alleles impact on affective personality traits and startle reactivity but not on cognition or gating in healthy males. *Bipolar Disorders* **13,** 250–259 (2011).
78. Bader, P. L. *et al.* Mouse model of Timothy syndrome recapitulates triad of autistic traits. *Proc. Natl. Acad. Sci. U.S.A.* **108,** 15432–15437 (2011).
79. Lee, A. S. *et al.* Forebrain elimination of cacna1c mediates anxiety-like behavior in mice. *Nat.Neurosci* **17,** 1054–1055 (2012).
80. Dao, D. T. *et al.* Mood Disorder Susceptibility Gene CACNA1C Modifies Mood-Related Behaviors in Mice and Interacts with Sex to Influence Behavior in Mice and Diagnosis in Humans. *Biological Psychiatry* **68,** 801–810 (2010).
81. Dedic, N. *et al.* Cross-disorder risk gene CACNA1C differentially modulates susceptibility to psychiatric disorders during development and adulthood. *Nat.Neurosci* **23,** 533–543 (2018).
82. Crider, A. *et al.* Complement component 3a receptor deficiency attenuates chronic stress-induced monocyte infiltration and depressive-like behavior. *Brain, Behavior, and Immunity* **70,** 246–256 (2018).
83. Sellgren, C. M. *et al.* Increased synapse elimination by microglia in schizophrenia patient-derived models of synaptic pruning. *Nat.Neurosci*, ***22,*** 374-385, (2019).
84. Wang, Y. *et al.* A role for complement in antibody-mediated inflammation: C5-deficient DBA/1 mice are resistant to collagen-induced arthritis. *J. Immunol.* **164,** 4340–4347 (2000).

85. Mikaelsson, M. A., Constancia, M. C. A., Dent, C. L., Wilkinson, L. S. & Humby, T. Placental programming of anxiety in adulthood revealed by Igf2-null models. *Nature Communications* **4,** 1–9 (2013).
86. Molewijk, H. E., van der Poel, A. M. & Olivier, B. The ambivalent behaviour 'stretched approach posture' in the rat as a paradigm to characterize anxiolytic drugs. *Psychopharmacology* **121,** 81–90, (1995).
87. Mackintosh, J. H. & Grant, E. C. A Comparison of the Social Postures of Some Common Laboratory Rodents. *Behaviour* **21,** 246–259 (1963).
88. Kleiber, M. Body size and metabolism. *Hilgardia Journal of Agricultural Science,* **6,** 315-353 (1932).
89. Dickmeis, T. Glucocorticoids and the circadian clock. *Journal of Endocrinology* **200,** 3–22 (2008).
90. Livak, K. J. & Schmittgen, T. D. Analysis of Relative Gene Expression Data Using Real-Time Quantitative PCR and the 2−ΔΔCT Method. *Methods* **25,** 402–408 (2001).
91. Wright, S. P. Adjusted p-values for simultaneous inference. *Biometrics* **48,** 1005–1013 (1992).

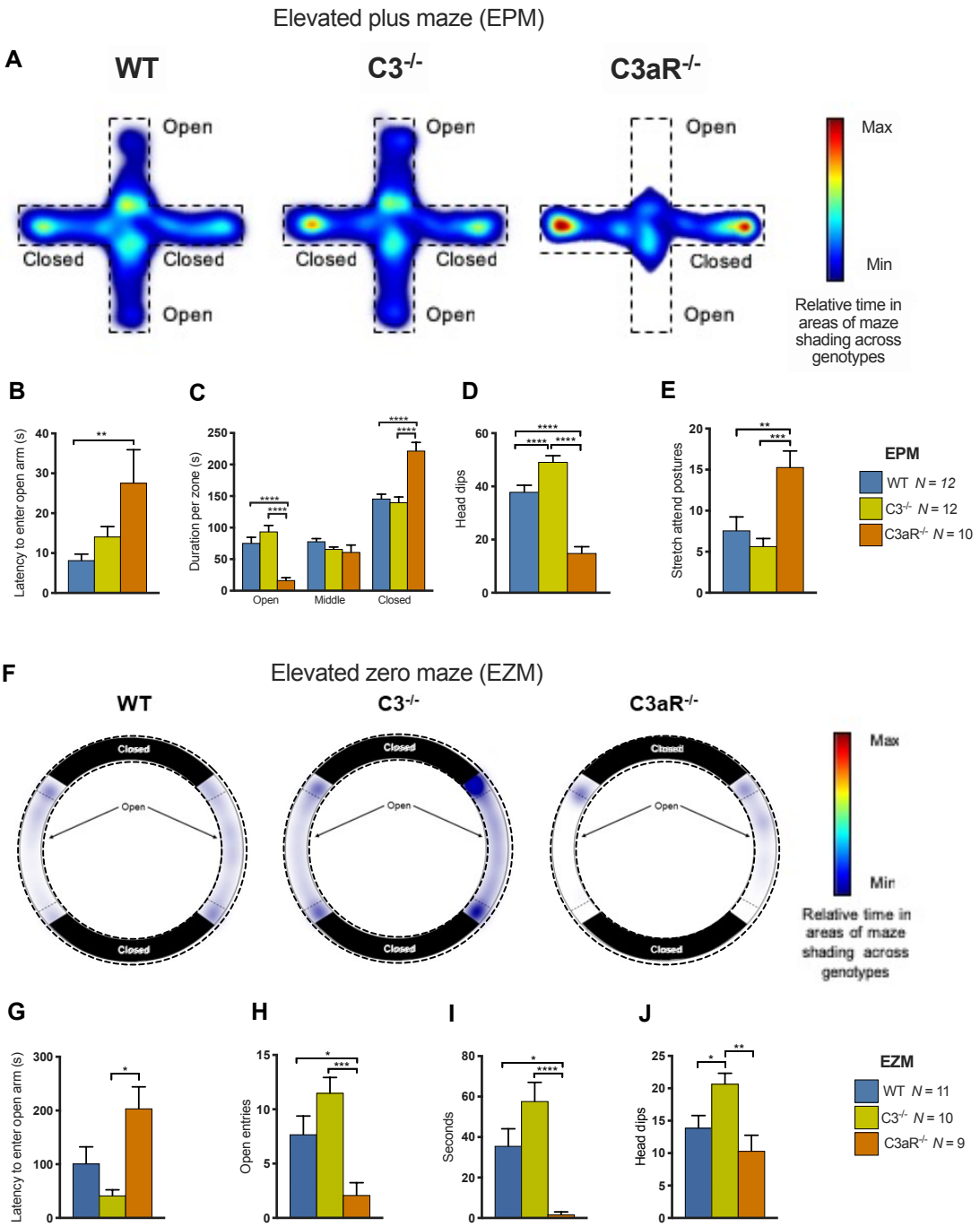

Figure 1. *C3aR*$^{-/-}$, but not *C3*$^{-/-}$ mice show increased anxiety-like behaviour in the elevated plus maze (EPM;A-E) and elevated zero maze (EZM;F-J). (A) Heatmaps displaying relative time per zone of the EPM across genotypes **(B)** Latency to first open arm visit; wildtype 8.21±1.53s, *C3*$^{-/-}$ 14.1±2.52s, *C3aR*$^{-/-}$ 27.6±8.31s, (H_2=10.5, p=0.005). *Post hoc* tests demonstrated that *C3aR*$^{-/-}$ mice took significantly longer to

967 first enter the open arms than wildtype mice (p=0.0045). **(C)** *C3aR*$^{-/-}$ mice distributed
968 their time across the EPM differently to wildtype and *C3*$^{-/-}$ mice (GENOTYPE×ZONE,
969 $F_{4,62}$=17.7, p=0.0001) spending less time in the open arms (*C3aR*$^{-/-}$ 16.70±3.73s vs.
970 wildtype 75.78±8.86s, p<0.0001, *C3aR*$^{-/-}$ vs. *C3*$^{-/-}$ 93.86±9.59s p<0.0001) and
971 significantly more time in the closed arms (*C3aR*$^{-/-}$ 221.88±12.06s vs. wildtype
972 146.01±7.01s, p<0.0001, and *C3*$^{-/-}$ 140.04±8.61s p<0.0001). **(D)** *C3aR*$^{-/-}$ (14.90±2.22)
973 mice performed significantly fewer head dips than wildtype (37.92±2.53, p<0.0001)
974 and *C3*$^{-/-}$ mice (49.17±2.37, p<0.0001), whereas *C3*$^{-/-}$ mice performed significantly
975 more head dips than wildtype mice (p=0.0061; overall ANOVA $F_{2,31}$=48.0, p<0.0001).
976 **(E)** *C3aR*$^{-/-}$ mice performed significantly more stretch attend postures (SAPs;
977 15.30±1.80) than wildtype (7.58±1.66, p=0.0042) and *C3*$^{-/-}$ mice (5.67±0.94, p=0.0004;
978 overall ANOVA $F_{2,31}$=10.3, p=0.0004). **(F)** Heatmaps displaying relative exploration of
979 the open segments of the elevated zero maze, across genotypes. Note that due to the
980 height of the walls in the closed regions it was not possible to track mice or observe
981 ethological behaviours such as grooming or SAPs. **(G)** There was a significant
982 difference in the latency to first enter the open arms (wildtype 101.00±31.00s, *C3*$^{-/-}$
983 42.00±2.52s, *C3aR*$^{-/-}$ 204.00±40.40s, H_2=8.13, p=0.0171). *Post hoc* tests revealed
984 that *C3aR*$^{-/-}$ mice took significantly longer than *C3*$^{-/-}$ mice to initially enter the open
985 region (p=0.0140). **(H)** The number of entries made to open regions differed between
986 genotypes (wildtype 7.69±1.69, *C3*$^{-/-}$ 11.5±1.43s, *C3aR*$^{-/-}$ 2.10±1.15, $F_{2,30}$=8.96,
987 p=0.0009). *C3aR*$^{-/-}$ mice made significantly fewer entries to the open areas than
988 wildtype (p=0.0324) and *C3*$^{-/-}$ mice (p=0.0006) and **(I)** spent significantly less time on
989 the open arms (1.77±1.29) compared to wildtype (35.7±8.43s, p=0.0132) and *C3*$^{-/-}$
990 (57.7±9.32s, p<0.0001; overall Kruskal-Wallis test H_2=19.2, p<0.0001). **(J)** *C3*$^{-/-}$ mice

991 performed significantly more head dips (20.7±1.62) than wildtype (13.9±1.89,
992 p=0.048) and *C3aR*$^{-/-}$ mice (10.3±2.42, p=0.0034; overall ANOVA
993 $F_{2,27}$=6.86,p=0.0039). Data are mean ± S.E.M. *, **, *** and **** represent p≤0.05,
994 p≤0.01, p≤0.001 and p≤0.0001 for *post-hoc* genotype comparisons, respectively.

995
996
997
998
999
1000
1001
1002
1003
1004
1005
1006
1007
1008
1009
1010
1011
1012
1013
1014
1015
1016
1017
1018
1019
1020
1021
1022
1023
1024
1025
1026

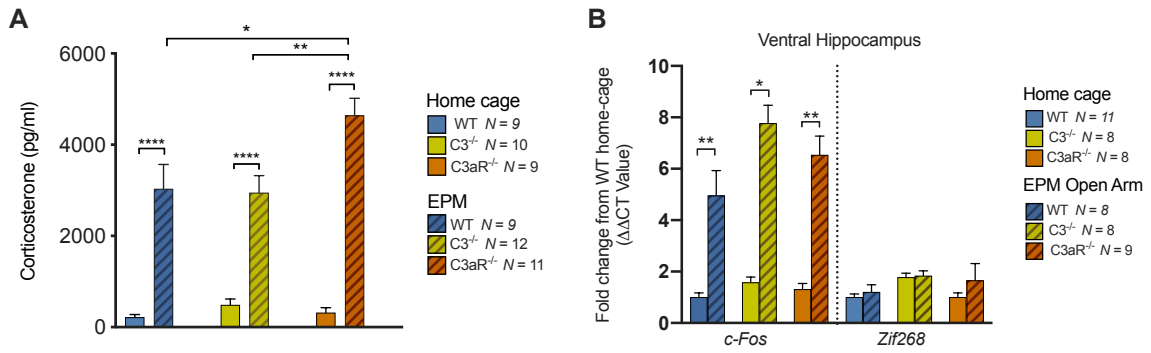

Figure 2. Neuroendocrine response and neuronal activation following exposure to the elevated plus maze (A) 5-minute exposure to the EPM significantly elevated corticosterone in all genotypes (main effect of CONDITION, $F_{1,54}$=143, p<0.0001; baseline 344.66±63.70 vs. EPM 3553.84±274.13). There was a significant GENOTYPE × CONDITION interaction ($F_{2,54}$=4.64, p=0.0138). *Post hoc* analysis showed that after the EPM, *C3aR*$^{-/-}$ mice demonstrated significantly higher corticosterone levels (4640.27±376.13) than wildtype (3033.78±535.06, p=0.0127) and *C3*$^{-/-}$ mice (2948.00±374.87, p=0.0032). *Post hoc* tests also indicated that there were no baseline differences between genotypes (wildtype 216.54±63.2 vs. *C3aR*$^{-/-}$ 316.17±111.60 p>0.9999, wildtype vs. *C3*$^{-/-}$ p=0.9927, and *C3*$^{-/-}$ 485.60±130.35 vs.*C3aR*$^{-/-}$ mice p=0.9992). **(B)** A separate group of animals were taken from their home-cages and culled immediately or placed on the open arm of the EPM for 5 minutes and culled 25 minutes later. *c-Fos* mRNA was significantly upregulated after exposure to the EPM across genotypes (main effect of CONDITION, $F_{1,46}$=45.4, p<0.0001). There was no significant main effect of GENOTYPE ($F_{2,46}$=1.27, p=0.2894) and no CONDITION × GENOTYPE interaction ($F_{2,46}$=0.0004, p=0.9996). *Zif268* mRNA was not altered in EPM exposed animals, nor between genotypes. Data represent mean + S.E.M or fold change from wildtype home-cage + SEM. *, **, and

1048 **** represent $p \leq 0.05$, $p \leq 0.01$ and $p \leq 0.0001$ for *post-hoc* genotype comparisons,

1049 respectively.

1050
1051
1052
1053
1054
1055
1056
1057
1058
1059
1060
1061
1062
1063
1064
1065
1066

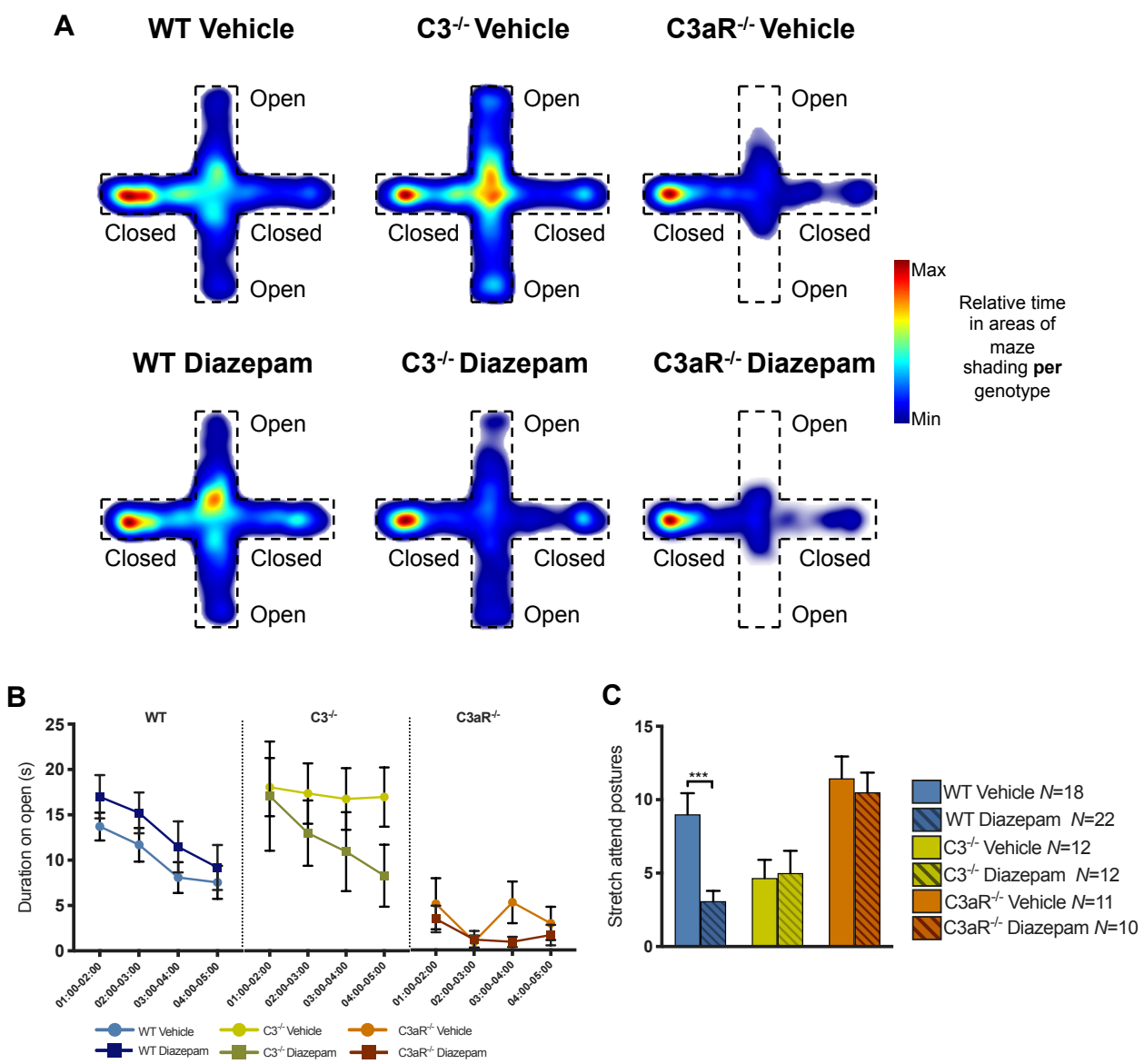

Figure 3. Altered sensitivity to diazepam in *C3aR*$^{-/-}$ and *C3*$^{-/-}$ mice. Behaviourally naïve mice were treated with either diazepam (2mg/kg, i.p) or vehicle injections once daily for 2 days and then 30 minutes prior to testing. (**A**) Heatmaps demonstrating duration spent in zones of the maze by vehicle treated and diazepam treated animals **(B)** Plots showing duration spent on open arms in 1-minute time bins (start-01:00 was excluded due to effect of diazepam in delaying initial entry to open arms across genotypes, see Supplementary Figure 4a). There was a trend for wildtype diazepam treated animals to spend more time on the open arms throughout the task

1077 although this did not reach significance (main effect of DRUG, $F_{1,38}$=1.41, p=0.2462).
1078 In *C3*$^{-/-}$ mice there was a strong tendency for drug treated animals to explore the
1079 open arms less than vehicle treated *C3*$^{-/-}$ mice (main effect of DRUG, $F_{1,22}$=1.25,
1080 p=0.2764). A similar, though less pronounced pattern was seen in *C3aR*$^{-/-}$ mice
1081 (main effect of DRUG, $F_{1,19}$=1.55, p=0.2284) **(C)** There were genotype differences in
1082 SAPs (main effect of GENOTYPE, $F_{2,79}$=10.7, p<0.0001), a main effect of DRUG
1083 ($F_{1,79}$=4.13, p=0.0454) and a significant GENOTYPE × DRUG interaction ($F_{2,79}$=4.64,
1084 p=0.0138). *Post hoc* tests showed that diazepam significantly reduced the number of
1085 SAPs in wildtype mice only (wildtype vehicle 9.00±1.44 vs. wildtype diazepam
1086 3.09±0.71, p=0.0006, *C3*$^{-/-}$ vehicle 4.67±1.24 vs. *C3*$^{-/-}$ diazepam 5.00±1.51,
1087 p=0.9975, *C3aR*$^{-/-}$ vehicle 11.45±1.49 vs. *C3aR*$^{-/-}$ diazepam 10.50±1.34, p=0.9558).
1088 Data are mean + S.E.M. *, **, and *** represent p≤0.05, p≤0.01 and p≤0.001 for
1089 *post-hoc* genotype comparisons, respectively.

1090
1091
1092
1093
1094
1095
1096
1097
1098
1099
1100
1101
1102

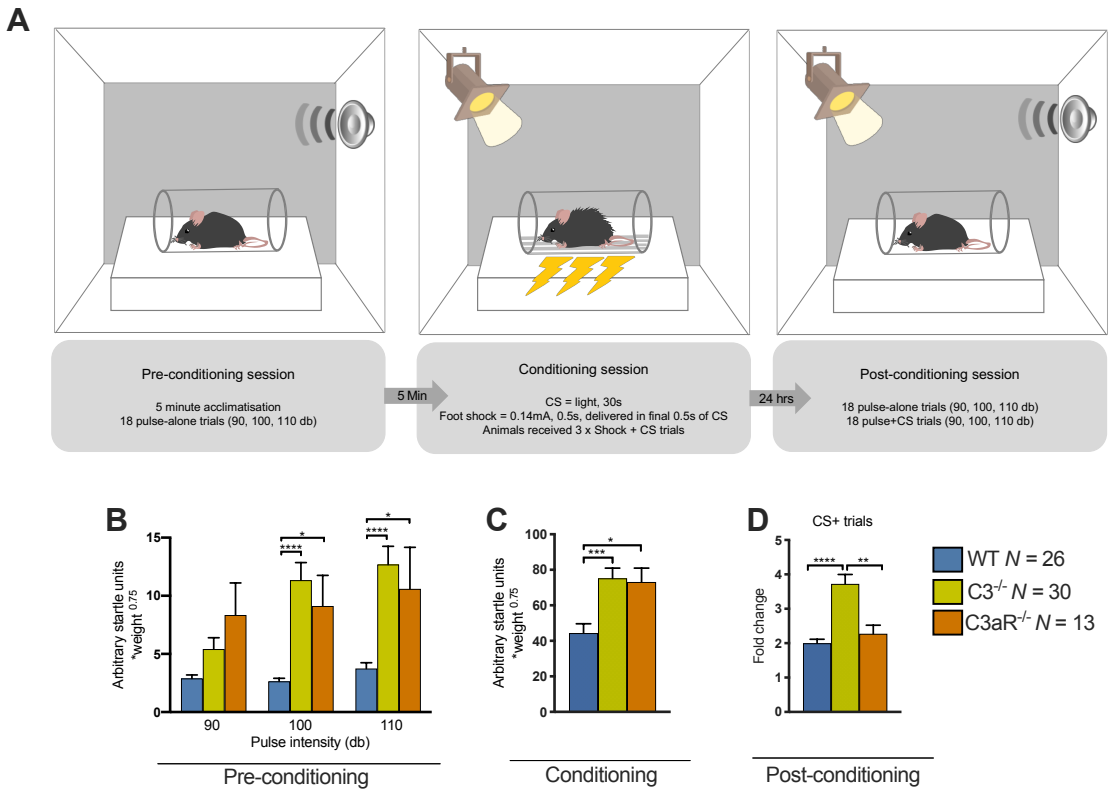

Figure 4. Enhanced fear-potentiated startle in *C3*$^{-/-}$ but not *C3aR*$^{-/-}$ mice. (A) Flow chart depicting the FPS protocol used, which took place in three separate sessions over two consecutive days. Baseline startle reactivity to a range of pulse intensities was assessed in the pre-conditioning session, immediately preceding the conditioning session in which a visual stimulus (light) was paired with 3 weak foot shocks. 24 hours later, subjects were re-introduced to the same chamber and startle reactivity was compared between pulse-alone trials and pulse+CS trials to determine the degree of FPS. On all trials, the peak startle response was recorded and normalised for body weight differences using Kleiber's 0.75 mass exponent, and fold-changes calculated. **(B)** There was a significant main effect of GENOTYPE ($F_{2,66}$=9.04, p=0.0003) and a significant GENOTYPE × STIMULUS INTENSITY interaction ($F_{4,132}$=7.55, p<0.0001). *C3*$^{-/-}$ and *C3aR*$^{-/-}$ mice demonstrated increased levels of startle responding relative to wildtype mice at 100dB (*C3*$^{-/-}$ 11.34±1.51 vs. wildtype 2.63±0.26, p<0.0001, *C3aR*$^{-/-}$

1118 9.12±2.63 vs. wildtype p=0.0174) and 110dB (*C3*$^{-/-}$ 12.69±1.55 vs. wildtype 3.74±0.50,
1119 p<0.0001, *C3aR*$^{-/-}$ 10.58±3.58 vs. wildtype p=0.0111) **(C)** *C3*$^{-/-}$ and *C3aR*$^{-/-}$ mice also
1120 showed increased startle responding to the footshock+CS (*C3*$^{-/-}$ 75.18±5.73, *C3aR*$^{-/-}$
1121 73.14±7.78) pairings relative to wildtype mice (44.34±5.29, *C3*$^{-/-}$ vs. wildtype p=0.0006,
1122 *C3aR*$^{-/-}$ vs. wildtype p=0.0137, overall ANOVA $F_{2,66}$=8.7, p=0.0004), although it should
1123 be noted that responses were much greater to these stimuli in all mice than to the
1124 startle stimuli in the pre-conditioning session. **(D)** In the post-conditioning session, all
1125 mice demonstrated increases to the pulse+CS stimuli in comparison to pulse-alone
1126 stimuli, as demonstrated by the fold-change increase in startle responding, however,
1127 this effect was significantly increased in *C3*$^{-/-}$ mice (3.72±0.27) relative to wildtype
1128 (1.99±0.11, p<0.0001) and *C3aR*$^{-/-}$ mice (2.27±0.24, p=0.0056, overall Kruskal-Wallis
1129 test H_2=27.7, p<0.0001). Data are mean + S.E.M. *, **, *** and **** represent p≤0.05,
1130 p≤0.01, p≤0.001 and p≤0.0001 for *post-hoc* genotype comparisons, respectively.

1131
1132
1133
1134
1135
1136
1137
1138

1139

1140

1141

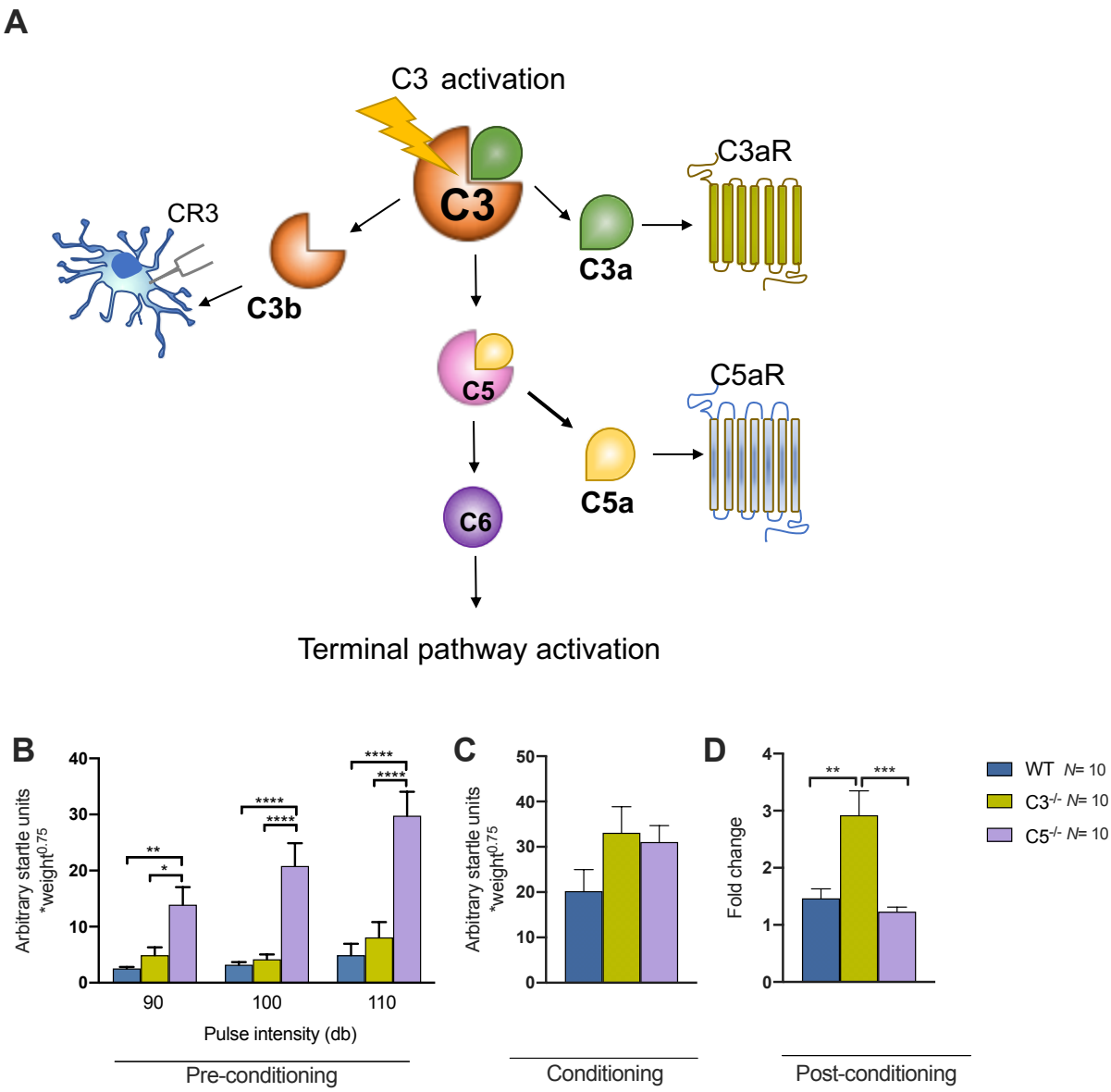

Figure 5. Pathways underlying fear learning phenotypes in *C3*$^{-/-}$ mice (A) C3 activation leads to generation of cleavage fragments C3a and C3b. The former signals via C3aR whereas the latter signals via complement receptor 3 (CR3). C3b is also necessary for forming the convertase enzyme that cleaves C5. Upon cleavage, C5 generates the fragments C5a and C5b (not shown). C5a signals via the C5aR, whereas C5b propagates activity of the terminal complement pathway via C6. Since C3 cannot be activated in *C3*$^{-/-}$ mice, the action of all these pathways (C3a/C3aR, C3b/CR3, C5a/C5aR, terminal pathway) is absent. By using *C5*$^{-/-}$ mice, which lack

1151 C5a/C5aR and terminal pathway activity, we examined whether lack of C3b/CR3,
1152 C5a/C5aR or the terminal pathway was responsible for fear learning phenotypes in
1153 *C3*$^{-/-}$ mice. **(B)** In the pre-conditioning session there were significant main effects of
1154 GENOTYPE ($F_{2,27}$=18.4, p<0.0001) and STIMULUS INTENSITY ($F_{2,54}$=19.0,
1155 p<0.0001) and a significant GENOTYPE × STIMULUS INTENSITY interaction
1156 ($F_{4,54}$=7.00, p<0.0001). *C5*$^{-/-}$ mice demonstrated increased levels of startle responding
1157 relative to wildtype and *C3*$^{-/-}$ mice at all stimulus intensities (90dB; WT 2.55±0.26 vs.
1158 *C5*$^{-/-}$ 13.92±3.14, p=0.0069, *C3*$^{-/-}$ 4.92±1.40 vs. *C5*$^{-/-}$ p=0.0405, WT vs. *C3*$^{-/-}$ p=0.7919;
1159 100dB; WT 3.23±0.45 vs. *C5*$^{-/-}$ 20.83±4.07, p<0.0001, *C3*$^{-/-}$ 4.924.17±0.88 vs. *C5*$^{-/-}$
1160 p<0.0001, WT vs. *C3*$^{-/-}$ p=0.9639; 110dB; WT 4.92±2.03 vs. *C5*$^{-/-}$ 29.78±4.29,
1161 p<0.0001, *C3*$^{-/-}$ 8.07±2.76 vs. *C5*$^{-/-}$ p<0.0001, WT vs. *C3*$^{-/-}$ p=0.6643). **(C)** There were
1162 no significant differences in startle responses to the footshock+CS pairings during the
1163 conditioning session (WT 20.23±4.76, *C3*$^{-/-}$ 33.10±5.74, *C5*$^{-/-}$ 31.08±3.59, $F_{2,27}$=2.10,
1164 p=0.1421). **(D)** In the post-conditioning session, all mice demonstrated increases to
1165 the pulse+CS stimuli in comparison to pulse-alone stimuli, as demonstrated by the
1166 fold-change increase in startle responding, however, this effect was again significantly
1167 increased only in *C3*$^{-/-}$ mice (2.92±0.43) relative to wildtype (1.47±0.17, p=0.0020) and
1168 *C5*$^{-/-}$ mice (1.23±0.08, p=0.0004, overall ANOVA $F_{2,27}$=11.5, p=0.0002). Data
1169 represent mean + S.E.M. *, **, *** and **** represent p≤0.05, p≤0.01, p≤0.001 and
1170 p≤0.0001 for *post-hoc* genotype comparisons, respectively.
1171
1172
1173

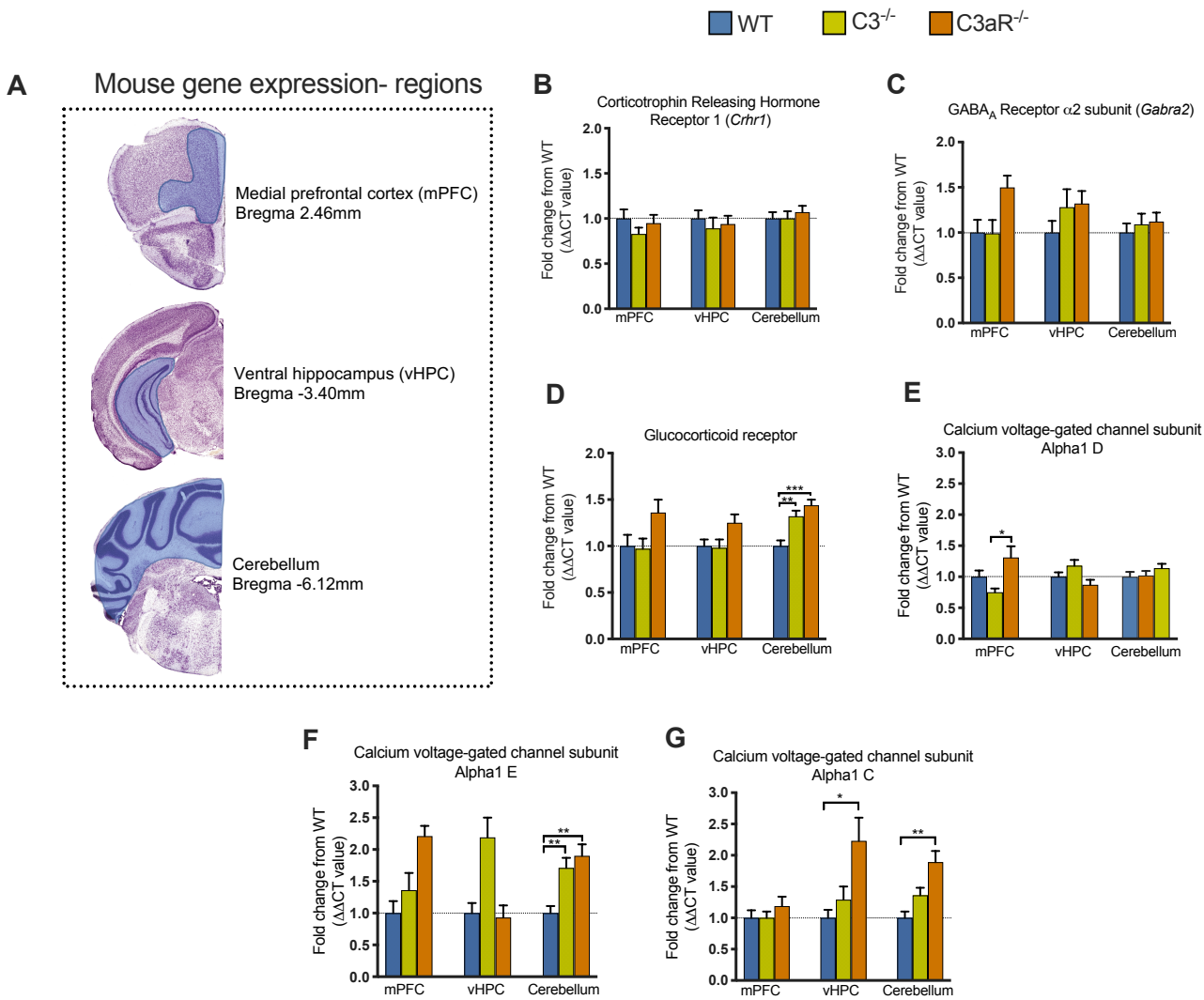

Figure 6. mRNA expression of stress and anxiety related genes. (A) Animals were culled and the medial prefrontal cortex (mPFC), ventral hippocampus (vHPC) and cerebellum were dissected. **(B)** There were no significant differences in the expression of Corticotrophin releasing hormone receptor 1 (*Crhr1*) in any region, across genotypes (mPFC $F_{2,53}$=0.587, p=0.5597, N wildtype=20, *C3*$^{-/-}$=17, *C3aR*$^{-/-}$= 19; vHPC $F_{2,49}$=0.169, p=0.8450, N WT=20, *C3*$^{-/-}$=15, *C3aR*$^{-/-}$= 17; cerebellum $F_{2,47}$=0.0482, p=0.8346, N WT=19, *C3*$^{-/-}$=17, *C3aR*$^{-/-}$= 14). **(C)** There were also no significant changes in the expression of the $GABA_A$ receptor α2 subunit (*Gabra2*) in any region, across genotypes (mPFC H_2=1.04, p=0.5939, N wildtype=20, *C3*$^{-/-}$=19, *C3aR*$^{-/-}$= 16; vHPC $F_{2,49}$=0.721, p=0.4914, N WT=20, *C3*$^{-/-}$=13, *C3aR*$^{-/-}$= 19; cerebellum

1185 $F_{2,47}$=0.221, p=0.8026, N WT=18, *C3*$^{-/-}$=17, *C3aR*$^{-/-}$= 15). **(D)** Expression of the
1186 glucocorticoid receptor (*Nr3c1*) was significantly increased in the cerebellum of both
1187 *C3*$^{-/-}$ and *C3aR*$^{-/-}$ groups ($F_{2,61}$=10.3, p=0.0002, *C3*$^{-/-}$ vs. wildtype p=0.0023, *C3aR*$^{-/-}$ vs.
1188 wildtype p=0.0002, N wildtype=19, *C3*$^{-/-}$=20, *C3aR*$^{-/-}$= 15). There were trends towards
1189 increased expression of the glucocorticoid receptor gene *Nr3c1* in the mPFC and
1190 vHPC of *C3aR*$^{-/-}$ mice but these were not significant (mPFC; $F_{2,56}$=1.33, p=0.2723, N
1191 wildtype=20, *C3*$^{-/-}$=20, *C3aR*$^{-/-}$= 19, vHPC; $F_{2,62}$=1.11, p=0.3345, N wildtype=23, *C3*$^{-/-}$
1192 =20, *C3aR*$^{-/-}$= 22). **(E)** Calcium voltage-gated channel subunit Alpha 1d (*Cacna1d*)
1193 expression was changed in the mPFC ($F_{2,36}$=7.52, p=0.0407) owing to altered
1194 expression between *C3*$^{-/-}$ and *C3aR*$^{-/-}$ mice (p=0.0314; N wildtype=11, *C3*$^{-/-}$=13, *C3aR*$^{-}$
1195 $^{/-}$= 15). There were no differences in the vHPC ($F_{2,31}$=2.27, p=0.1199, N wildtype=14,
1196 *C3*$^{-/-}$=10, *C3aR*$^{-/-}$= 10) or cerebellum ($F_{1,39}$=0.648, p=0.5286, N wildtype=14, *C3*$^{-/-}$=16,
1197 *C3aR*$^{-/-}$= 12). **(F)** Expression of the Calcium voltage-gated channel subunit Alpha 1e
1198 (*Cacna1e*) was significantly upregulated in the cerebellum of both knockouts
1199 ($F_{2,39}$=7.52, p=0.0017, wildtype vs. *C3*$^{-/-}$ p=0.0082, wildtype vs. *C3aR*$^{-/-}$ p=0.0032; N
1200 wildtype=14, *C3*$^{-/-}$=16, *C3aR*$^{-/-}$= 12). There were borderline significant changes in
1201 expression in the vHPC ($F_{2,32}$=3.15, p=0.0565, N wildtype=14, *C3*$^{-/-}$=11, *C3aR*$^{-/-}$= 10)
1202 and no significant changes in the mPFC (H_2=3.43, p=0.1802, N wildtype=11, *C3*$^{-/-}$=12,
1203 *C3aR*$^{-/-}$= 15).**(G)** Expression levels of the Calcium voltage-gated channel subunit
1204 Alpha 1c (*Cacna1c*) were significantly increased in *C3aR*$^{-/-}$ mice in a regionally specific
1205 manner in the vHPC ($F_{2,47}$=3.20, p=0.0496, *C3*$^{-/-}$ vs. wildtype p=0.6895, *C3aR*$^{-/-}$ vs.
1206 wildtype p=0.0295, N wildtype=21, *C3*$^{-/-}$=13, *C3aR*$^{-/-}$= 16) and the cerebellum
1207 ($F_{2,54}$=5.84, p=0.0051, *C3*$^{-/-}$ vs. wildtype p=0.1613, *C3aR*$^{-/-}$ vs. wildtype p=0.0024, N
1208 wildtype=20, *C3*$^{-/-}$=20, *C3aR*$^{-/-}$= 17). There were no significant changes in the mPFC
1209 ($F_{2,52}$=1.04, p=0.5939, N wildtype=20, *C3*$^{-/-}$=19, *C3aR*$^{-/-}$= 16). Data represent fold

1210 change from wildtype + SEM. *, **, *** represent $p \leq 0.05$, $p \leq 0.01$ and $p \leq 0.001$ for *post-*

1211 *hoc* genotype comparisons, respectively.

1212

1213

1214

1215

1216

1217

1218

1219

1220

1221